MATRIX ISOLATED INFRARED SPECTROSCOPY OF CARBON CLUSTERS

BY

T. M. CHANDRASEKHAR

A DISSERTATION PRESENTED TO THE GRADUATE SCHOOL
OF THE UNIVERSITY OF FLORIDA IN PARTIAL
FULFILLMENT OF THE REQUIREMENTS FOR THE
DEGREE OF DOCTOR OF PHILOSOPHY

UNIVERSITY OF FLORIDA

1990

To my parents.

ACKNOWLEDGEMENTS

I would like to thank my advisor, Professor Martin Vala, for his support, encouragement and guidance through my five years of study in his group.

I also wish to express my gratitude to Dr. Jan Szczepanski for his invaluable help with the experiments and Prof. Weltner for generously lending us the Nd-YAG laser that made this work possible. Thanks are also due to Dr. Cliff Johnston for making available the Microvax computer and other resources in his laboratory.

The friendship and assistanse of my colleagues, Dennis, Bill and Bob, will always be valued by the author. I also want to express my appreciation for the craftsmanship and expertise of the staff of the mechanical, glass and electronics workshops.

Finally, my parents also deserve a great deal of credit for allowing me to pursue my interest in chemistry. Their guidance and support over the years has enabled me to reach this point.

TABLE OF CONTENTS

		Page
ACKNOWLEDGEMENTS		iii
LIST OF TABLES		vi
LIST OF FIGURES		vii
ABSTRACT		ix
CHAPTERS		
I	INTRODUCTION	1
	Small Clusters: C_2-C_4	2
	Small Clusters: C_5-C_9	8
	Large Clusters	10
	Ionic Clusters	19
	Carbon Clusters and Soot Formation	21
II	EXPERIMENTAL	23
	Experimental Approach	24
	Matrix Isolation Apparatus	31
	Carbon Cluster Preparation	36
	Instrumentation	42
III	THE C_5 CLUSTER	44
	Introduction	44
	Results	46
	Normal Coordinate Analysis	52
	Discussion	55
	Conclusion	59
IV	THE C_6 AND C_8 CLUSTERS	60
	Introduction	60
	Results	62
	Normal Coordinate Analysis	76
	Discussion	80
	Conclusion	83

V THE IONIC C_5^+ CLUSTER..... 84

Introduction..... 84
Experimental Procedure..... 88
Results..... 89
Discussion..... 102
Conclusion..... 105

VI CONCLUSIONS AND FUTURE WORK..... 112
Future Work..... 112
Concluding Remarks..... 115

REFERENCES..... 116

BIOGRAPHICAL SKETCH..... 127

LIST OF TABLES

Table		Page
1	Isotopomer Stretching Frequencies for linear C_5....	56
2	Observed and Calculated Isotopomer Stretching Frequencies for linear C_5.....	57
3	Expected Number of Isotopomers for Linear Carbon Clusters.....	66
4	Observed and Calculated Isotopomer Stretching Frequencies for Chain-like C_6 in an Argon Matrix.....	77
5	Observed and Calculated Isotopomer Stretching Frequencies for Linear C_6 in an Argon Matrix.....	78
6	Expected Number of Isotopomers for Linear and Cyclic Carbon Clusters.....	96
7	Calculated Frequencies for Tetrahedral C_4 for $\theta = 25°$.....	98
8	Calculated Fits for Pyramidal C_4.....	99
9	Observed and Calculated Isotopomer Stretching Frequencies for Cyclic C_5^+ in an Argon Matrix.....	101

LIST OF FIGURES

Figure		Page
2.1	Isotopomers of C_3.....	27
	(a) Linear structure.....	27
	(b) Cyclic structure.....	27
2.2	Infrared spectrum in the 2070-1930 cm^{-1} region of laser-ablated ^{12}C products (lower spectrum) and ^{12}C:^{13}C isotopically-mixed products (upper spectrum) in unannealed argon matrices at 12 K showing the six isotopomeric bands....	30
2.3	Cryostat and furnace assembly.....	33
2.4	Sample degassing setup	
	(a) Furnace assembly.....	35
	(b) Knudsen cell.....	35
2.5	Experimental setup for the matrix isolation of laser-ablated carbon in argon.....	39
2.6	Experimental setup for distinguishing between ions and neutrals in the argon matrix.....	41
3.1	Infrared spectrum of the products of laser-ablated ^{12}C in an unannealed argon matrix.....	48
3.2	Infrared spectra of the 2180-2070 cm^{-1} region of laser vaporized graphite in an argon matrix (12 K). Top panel: 1:1 mixture of ^{12}C:^{13}C; black dots indicate bands due to isotopomers of linear C_5 (cf. Table 1); indicated 2164 cm^{-1} band is from $^{12}C_5$ and 2079.5 cm^{-1} from $^{13}C_5$. Bottom panel: pure ^{12}C graphite; 2128 cm^{-1} band has been ascribed to $^{12}C9$.....	51
4.1	Difference spectrum [annealed (35 K) - unannealed] of ^{12}C laser-ablation products in an argon matrix.....	65

4.2 Infrared spectra over the 2070-1930 cm^{-1} range of ^{12}C products (lower spectrum) and ^{12}C:^{13}C isotopically mixed products (upper spectrum) isolated in unannealed argon matrices at 12 K showing the six C_3 isotopomeric bands..... 68

4.3 Infrared spectra over the 1980-1870 cm^{-1} range of ^{12}C products (lower spectrum) and ^{12}C:^{13}C isotopically-mixed products (upper spectrum) isolated in unannealed argon matrices at 12 K showing the more prominent C_6 isotopomer bands (cf Table 5)..... 71

4.4 Infrared spectra over the 2000-1920 cm^{-1} range of ^{12}C products (lower) in an unannealed argon matrix. Upper spectrum shows the IR of the ^{12}C:^{13}C mixed productsin argon at 12 K after annealing to 35 K for 15 min. Note the increased density of bands compared to Figs. 4.2 and 4.3..... 73

5.1 Bottom spectrum: Infrared spectrum of ^{12}C products in an unannealed argon matrix at 12 K showing prominent 1998 cm^{-1} C_8 peak. Top spectrum: Infrared spectrum of products from a laser-vaporized 1:1 ^{12}C:^{13}C isotopic mixture in an annealed argon matrix at 12 K showing C_3 isotopomer peaks ( ) and cyclic C_5^+ isotopomeric peaks ( )..... 92

5.2 Left panel: Portion of infrared spectrum with +48.0 V. on the ring electrode during deposition showing the $^{12}C_5^+$ peak at 2052 cm^{-1} and neutral $^{12}C_3$ peak at 2039 cm^{-1}. Right panel: Portion of infrared spectrum with -48.0 V. on the ring electrode of an unannealed matrix of ^{12}C in argon at 12 K..... 94

5.3 Proposed mechanism for the formation of cyclic C_5^+..... 104

5.4 Proposed mechanism for the formation of the corannulene decaradical using cyclic C_5^+, C_2 and C_3 as precursors..... 107

5.5 Proposed structure of C_{60}(Buckminsterfullerene). 110

Abstract of Dissertation Presented to the Graduate School of the University of Florida in Partial Fulfillment of the Requirements for the Degree of Doctor of Philosophy

MATRIX ISOLATED INFRARED SPECTROSCOPY OF CARBON CLUSTERS

By

T. M. Chandrasekhar

May, 1990

Chairman: Martin T. Vala
Major Department: Chemistry

Infrared Spectroscopy is a powerful technique that can be used to determine the size and structure of matrix isolated clusters. It allows one to characterize the ground state geometry of the entrapped species by measuring the vibrational frequencies associated with the species. The approach used to identify the sizes and ground state geometries of the clusters identified is a variant of the well-known isotopic substitution method in infrared spectroscopy.

The method involves, first, the infrared spectral recording of the products of vaporized ^{12}C graphite, followed by the recording of products of a vaporized sample from a 1:1 mixture of ^{12}C:^{13}C powder. For a particular cluster size and geometry, all the isotopomeric structures possible can be expected if, during the laser vaporization process, the graphitic carbon is atomized and the atoms react to form clusters before deposition in the matrix. The number of isotopomers formed for any given cluster size is

dependent on the geometry of the cluster. Thus, the number of different isotopomeric infrared frequencies observed in the 1:1 mixed run is direct information on the geometry and size of the cluster. Generally, the number of isotopomeric bands does not lead to a unique choice of cluster size and geometry, but the choices are considerably narrowed. In order to collapse these choices to a final one, a normal coordinate analysis is performed. A good fit is effected when the deviation of the observed and predicted bands is small and the force constants used to obtain the fit are reasonable.

This method has been used to identify the infrared bands and determine the geometries of the C_5, C_6, C_8 and C_5^+ clusters. The 2164 cm^{-1}, 1998 cm^{-1}, 1952 cm^{-1} and 2052 cm^{-1} bands were assigned to the linear C_5, chain-like C_6, chain-like C_8 and cyclic C_5^+ clusters respectively.

CHAPTER I

INTRODUCTION

The chemistry and physics of clusters have long been recognized as being of importance in such diverse areas as catalysis and combustion.[1] Carbon clusters are also of astrophysical[2] interest since small clusters have been identified in comet tails and the atmospheres of stars.[3] A comprehensive review of the spectroscopy of carbon clusters has recently been submitted by Weltner and Van Zee.[4]

The study of carbon clusters has been greatly aided by the development of new technology and experimental techniques. Older studies which used thermal vaporization of graphite yield C, C_2 and C_3 as the dominant species.[5-8] Laser vaporization of graphite can produce a wide range of neutral and ionic clusters[9,10] from C_2 to C_{30}. Larger clusters, up to C_{100}, have been produced using laser vaporization and pulsed helium expansion sources.[11] Some of the background on carbon clusters will be reviewed in this chapter.

Small Clusters: C_2-C_4

Both C_2 and C_3 have been extensively studied and are well characterized.[4,12-19] They are ubiquitous molecules and have been detected in comets,[20] the atmospheres of cool carbon stars[21,22] and giant circumstellar shells.[23] They have also been detected in electrical discharges,[24] flames and explosions.[25]

The first spectroscopic observation of a cluster of carbon atoms was reported over a century ago by Huggins while investigating the spectra of comets.[26] The 405 nm band group that Huggins observed was subsequently reproduced in the laboratory by Herzberg in 1942 by an electrodeless discharge through methane[12] but was not correctly assigned to the linear C_3 molecule until Douglas reinvestigated the spectrum in 1951.[13] The absorption spectrum of C_3 was also observed by the flash photolysis of diacetylene,[27] diazomethane,[15a] and diazopropyne.[28] In addition to the difficulties in identifying the carrier of the band system, problems also arose in assigning the upper and lower electronic states. Douglas determined that the 405 nm band group arises from the C_3 molecule, which he determined to be linear in both the upper and lower electronic states. He was however unable to determine whether the transition was of $^1\Pi_u$-$^1\Sigma_g^+$ or $^1\Sigma_g^+$-$^1\Pi_u$ symmetry. Finally, in two papers published in 1963 and 1965, Gausset, Herzberg, Lagerqvist

and Rosen[15] analyzed several bands of the 405 nm band group, assigning the transition as $A^1\Pi_u \leftarrow X^1\Sigma_g^+$. They also determined the ground- and excited-state bending frequencies, observed a large ℓ-type doubling in the $X^1\Sigma_g^+$ state, and analyzed the $A^1\Pi_u$ state in terms of the Renner-Teller effect.

Lemire et al.[19] have recently reported a new band system in the 266-302 nm region by resonant two-photon ionization of jet-cooled C_3. They determined that these bands had $\Sigma_u^+ \leftarrow \Sigma_g^+$ vibronic symmetry, with all transitions originating from the lowest vibronic level of $X^1\Sigma_g^+$ C_3. They also concluded that the new band system(s) is(are) electric-dipole forbidden and tentatively assigned the upper state(s) as either a $^1\Pi_g$ or $^1\Delta_u$. Rohlfing and Goldsmith[29] have recently reported preliminary results on the stimulated emission pumping spectroscopy of jet-cooled C_3. They obtained dispersed fluorescence spectra for excitation of 13 vibronic bands of the $\Sigma_u^+ - \Sigma_g^+$ type. Kawaguchi, Matsumura, Kanamori and Hirota[30] have recently reported the observation of the ν_3 hot bands (011)-(010), (021)-(020) and the combination band (021)-(000) of C_3 by diode laser spectroscopy. The C_3 was produced by photolysis of allene or by an ac discharge in cyclopropane or furan.

Barger and Broida,[31] Bondybey and English,[32] and Weltner and coworkers[16,17] have obtained absorption spectra of C_3 in rare gas matrices. These low-temperature studies

resulted in the determination of the symmetric (ν_1) and antisymmetric (ν_3) stretching frequencies of C_3 in the $^1\Sigma_g^+$ ground state and the symmetric (ν_1) vibration in both the $A^1\Pi_u$ and $X^1\Sigma_g^+$ electronic states. It also extended the treatment of the Renner-Teller effect in the $A^1\Pi_u$ state. Weltner and McLeod[17] recorded the absorption spectrum of C_3 trapped in low-temperature neon, argon, and xenon matrices and reported the ν_3 antisymmetric stretching frequency to be 2038 cm^{-1} in the ground electronic state. Vaporization of 60% ^{13}C enriched samples of graphite produced six isotopomer bands in the infrared in the 2038-1959 cm^{-1} region. These bands were fit to a linear C_3 molecule and force constants obtained by them.

A linear structure for C_3 was also obtained by Goldring et al.[33] and Plesser, Vager and Naaman[34] by the Coulomb Explosion technique.[35,36] The experiment is highly sensitive to the bond angle and the data fitted well with an ensemble of linear C_3 molecules with the above vibrational frequencies in thermal equilibrium at 500 K. Recent theoretical work by Jones[37] confirmed the linear structure for C_3 and concluded that the C-C-C bond angle can be changed by a large amount from its equilibrium value, with a very small change in its energy or bond length.

The very low ground-state bending frequency of C_3 (~63 cm^{-1}) leads to large amplitude vibrational motion with bending angles up to 60° and therefore to deviations from

harmonic small-amplitude models. Quasilinear and quasiplanar molecules[38] involve large nuclear motions. This prompted Gausset et al.[15] to suggest that C_3 might not be linear in the ground state but that, if a slight potential maximum exists, it should be less than ν_2''. Hoffmann,[39] using extended Huckel theory, predicted that C_3 would be nonlinear with an equilibrium CCC angle of ~160° and a very small barrier of ~65 cm^{-1} at the linear state. However, later calculations by Peric-Radic et al.[40] using MRD-CI and by Jones[37] utilizing the parameter-free local spin density approximation predicted a linear structure for C_3. Jones predicted the ground state bending frequency to be 75 cm^{-1}.

C_2 is a well studied molecule: about 17 electronic states of the molecule have been identified so far. Huber and Herzberg[41] have tabulated the electronic, structural, and vibrational properties of C_2 known as of about 1977. Every year since then, there have been numerous papers identifying C_2 in some gaseous source and often adding to the detailed knowledge of its spectroscopy.

Some of the better studied electronic band systems studied to date are the Swan system[42-47] ($d^3\Pi_g - a^3\Pi_u$), the Phillips system[47-53,55] ($A^1\Pi_u - X^1\Sigma_g^+$), the Ballik-Ramsey system[52,54,55] ($b^3\Sigma_g - a^3\Pi_u$), the Fox-Herzberg system[54-57] ($e^3\Pi_g - a^3\Pi_u$), the Mulliken system[45,51,54,57] ($D^1\Sigma_u^+ - X^1\Sigma_g^+$), the Deslandres-d'Azambuja system[51,54,57] ($C^1\Pi_g - A^1\Pi_u$) and the Freymark system[54,57] ($E^1\Sigma_g^+ - A^1\Pi_u$).

Ab initio calculations of equilibrium geometries have been done by DeFrees et al.,[58] of excitation and dissociation energies by Raghavachari[59] and of geometries and spectroscopic constants by Rohlfing and Martin.[60] Franck-Condon factors have been calculated by several authors including Walvekar and Rama,[61] Brown,[62] and Kuzmenko and Chumak.[63] Partition functions and thermodynamic functions in the range of 1000 to 9000 K have been compiled by Sauval and Tatum[64] and Rossi, Maciel and Benevides-Soares[65] from the available molecular data.

Clementi and Clementi[66] has carried out ab initio SCF-LCAO calculation on C_4 and predicted a linear structure with a $^3\Sigma_g^-$ ground state. This corresponds to a cumulenic structure, as Pitzer and Clementi[67] had previously reported. Hoffmann[39], using extended Huckel theory also predicted a linear structure for C_4. A number of ab initio calculations have been performed by several groups[68-71] on C_4 with the chief contenders for ground state geometry being the triplet linear and singlet rhombic, bicyclic structures. Most of the calculations predicted the singlet rhombic form as slightly more stable with the difference between the two energies being about 5 kcal/mole.

However, a recent calculation by Bernholdt, Magers and Bartlett,[71] using various levels of coupled-cluster and many body perturbation theory predicted that both the linear and rhombic forms of C_4 are essentially isoenergetic.

Calculations on equilibrium vaporization indicated that entropy favors the linear form over the rhombic structure by a factor of seven to one. The vibrational frequencies, ESR hyperfine splitting parameters, ionization potentials and electron affinities of both molecules were also calculated. The IR-active frequencies of the linear form were calculated to be 1586 cm^{-1} (Σ_u^+) and 187 cm^{-1} (Π_u) respectively. Sanborn[72] has calculated the Σ_u^+ stretching frequency of linear C_4 to be 1700 cm^{-1}. Calculations by Martin, Francois and Gijbels[73] also assigned the experimentally observed 1544 cm^{-1} band to linear C_4.

Graham, Dismuke and Weltner[74] have generated C_4 by the photolytic dissociation of C_4H_2 and the evaporation of graphite, and trapped it at 4K in solid neon and argon. The C_4 was identified on the basis of optical and ESR studies. Two absorption bands at 520.1 nm and 469.9 nm were assigned to linear C_4 on the basis of annealing studies. These bands were observed to grow in a parallel fashion with the C_4 ESR signals upon repeated annealing up to 25 K. Warming above 30 K caused a loss of band intensity. More recent results on the ESR of C_4 by Cheung and Graham[75] suggested that C_4 had a chain-like, albeit slightly bent structure.

Small Clusters: C_5-C_9

The thermal vaporization of graphite[8,76] yields predominantly carbon atoms plus C_2 and C_3 atoms. Small amounts of larger clusters are also produced. Early theoretical work[39,66,67,77] predicted that all clusters containing up to ten carbon atoms should be linear. More refined recent calculations[68-71,78-80] have indicated that some ground state clusters with four or more atoms may not be linear. Raghavachari and Binkley[79] have calculated that odd carbon clusters have lowest energy linear structures while even carbon clusters should be cyclic.

Other recent theoretical work by Bernholc and Phillips[81] predicted that all clusters containing between 3 and about 9 atoms should be linear. Calculations on C_5 done by Ewing and Pfeiffer,[82-84] and Ott and Ray[85] predicted a ground state linear structure. Sanborn[72] has calculated the vibrational frequencies of linear C_5 and C_6. The IR-active Σ_u^+ vibrations were calculated to be 2210 cm^{-1} and 1430 cm^{-1} for C_5, and 2040 cm^{-1} and 1230 cm^{-1} for C_6. Recent theoretical studies, which include electron correlation effects, are now sufficiently powerful to predict with high accuracy the ground state vibrational frequencies of unknown molecules such as carbon clusters. These calculations generally predict frequencies that are 10% too high. For the infrared active ungerade modes, Raghavachari and Binkley[79]

calculate 2344 $cm^{-1}(\sigma_u)$, 1632 $cm^{-1}(\sigma_u)$, 648 $cm^{-1}(\pi_u)$ and 112 $cm^{-1}(\pi_u)$ for linear C_5 and 2184 $cm^{-1}(\sigma_u)$ and 1289 cm^{-1} (σ_u) for linear C_6. Infrared studies on matrix isolated carbon clusters done by Thompson, DeKock and Weltner[86] assigned the 1952 cm^{-1} and 1544 cm^{-1} band to linear $^{12}C_5$.

C_6 and C_8 were first detected by Drowart et al.[8] using mass spectrometry. Early calculations by Pitzer and Clementi[67] and Ewing and Pfeiffer[82] predicted linear structures for both molecules. MNDO calculations by Bernholc and Phillips[81] also predicted a linear structure. Ab initio studies by Raghavachari, Whiteside and Pople[80] found the cyclic singlet structure with six pi electrons (planar D_{3h}, ^1A) to be the ground state structure with the linear $^3\Sigma_g^-$ structure lying about 10 kcal/mole higher in energy. Other calculations by Ott and Ray[85] and Parasuk and Almlof[87] predicted a linear ground state structure for C_6.

Kratschmer, Sorg and Huffman[88] have recorded UV-VIS absorption spectra of carbon clusters in an argon matrix and assigned a series of bands in the 240 to 600 nm region to linear C_4 to C_9 clusters. Their assignments were as follows: C_4 (247 nm), C_5 (311 nm), C_6 (394 nm), C_7 (447 nm), C_8 (529 nm) and C_9 (586 nm). These bands were assigned to $\Sigma_u \leftarrow \Sigma_g$ transitions in linear molecules.

Thompson, DeKock and Weltner[86] have assigned the 1997 cm^{-1} and 1197 cm^{-1} bands to $^{12}C_6$. A recent ESR study of graphite vapour in argon and neon matrices by Van Zee et

al.[89] concluded that C_6, C_8, and C_{10} were linear and present in the matrices in their lowest $^3\Sigma$ states. They also found evidence for two forms of C_{10}, possibly two slightly bent isomers.

A new crystalline allotrope of carbon, "C_8", which is denser than diamond, has recently been claimed, following research on the plasma deposition of thin carbon films.[90] The reported structure consists of a body-centered cubic array of C_8 cubes, forming a lattice previously postulated by Burdett and Lee[91] and termed "supercubane". Johnson and Hoffmann[92] however believe that the new form of C_8 probably has the BC-8 structure, adopted by the high-pressure γ-Si allotrope. This conclusion was reached from extended Huckel band calculations and from discrepancies in the crystallographic analysis and unusual bond length distribution of the reported structure.[90]

Large Clusters

The mass spectrometric study of carbon clusters dates from the first work done by Hahn et al.[93,94] in 1942 in which species containing as many as 15 carbon atoms were observed. Prior to 1984, several workers[5,6,8,9,10] sucessfully produced and detected carbon cluster ions ranging in size up to 33 atoms.

Large C_n clusters ($n \geq 10$) were produced by the pulsed supersonic expansion of laser vaporized carbon in high pressure helium gas by Rohlfing, Cox and Kaldor.[11] The clusters were photoionized using a 193 nm or 248 nm ArF excimer laser and detected by a time-of-flight mass spectrometer (TOF-MS). The cluster distribution was found to be bimodal with both even and odd clusters being observed for C_n, $1 \leq n \leq 30$ and only even clusters C_{2n} for $20 \leq n \leq 90$. The observation of only C_{2n} clusters for large n was explained as being due to the laser induced transformation of graphite into "chunks" of a new, high temperature phase of carbon, the carbyne phase, composed of cross-linked acetylene-like linear chains $(-C\equiv C-)_n$.

When the graphite rod was pretreated with KOH, and the experiment repeated, clusters of the type K_2C_{2n} were observed with n = 3-12. This was presented as evidence that the clusters C_n for $1 \leq n \leq 24$ have linear chain structures. Ab initio calculations on linear carbon chains[95] predict that odd numbered clusters have singlet ground states while the even numbered clusters have triplet ground states in which most of the unpaired electron density resides on the terminal carbon atoms. These even numbered diradical species were thought to add a potassium atom to each end to form the K_2C_{2n} clusters with the structure $K\text{-}(C\equiv C)_n\text{-}K$. The formation of a whole series of K_2C_{2n} clusters was presented as proof that the potassium addition occurs after the formation of

the carbon clusters since addition during cluster growth would presumably terminate carbon chain formation.

Heath et al.[96] have studied the reactions of C_n carbon clusters up to n = 40 with small molecules like H_2, H_2O, NH_3 and CH_3CN and found that the initially formed even n species for n<24 are reactive radicals with linear carbon chain structures that can readily add H, N, or CN at the ends to form relatively stable polyynes or cyanopolyynes. The curious prominence of the C_{11}, C_{15}, C_{19}, and, to some extent, C_{23} (the $\Delta n = 4$ effect) was observed but could not be interpreted satisfactorily, although others[81b,97] have considered this as possible proof for the existence of ring structures.

Heath et al. and Rohlfing, Cox and Kaldor's conclusions are in marked contrast to the conclusions reached by McElvany and coworkers. They detected an abrupt change in the reactivity of C_n clusters (n = 3-30) with D_2 and O_2,[98] HCN[99] and small hydrocarbons like CH_4, C_2H_2 and C_2H_4[100] between n = 9 and 10. They interpreted this as the result of a structural change from linear to monocyclic rings in the cluster ions between n = 9 and 10. Similar conclusions were reached by Yang et al.[101] in UPS studies of negative carbon clusters in the 2-30-atom range. They found that in the 2-9-atom range, the even numbered chains had open shell electronic structures with high electron affinities while the odd chains had closed shell singlet ground states (for

the neutral) and substantially lower electron affinities. Clusters in the 10-29-atom range gave UPS patterns consistent with monocyclic ring structures. Calculations by Bernholc and Phillips[81] and Ott and Ray[85] support these conclusions and predict cyclic ground states for n>9.

Among the larger clusters, the C_{60} cluster has received much attention recently. Smalley and coworkers[102] repeated the experiment of Rohlfing et al and observed that the size distribution of the large even-numbered carbon clusters was extremely sensitive to vaporization conditions. When the helium carrier gas pressure and residence time in the nozzle were increased, C_{60} was found to account for more than 50% of all clusters observed. They also discovered that the C_{60} cluster was extremely inert and proposed that the extreme stability of the cluster could be accounted for by the formation of a closed spherical shell structure that had no reactive edges. The proposed structure for C_{60}, dubbed Buckminsterfullerene was that of a soccerball: 12 pentagons and 20 hexagons arrayed on the surface of a sphere with icosahedral symmetry.

A study on the reactivity of carbon clusters with small molecules such as NO, CO, H_2, O_2, SO_2 and NH_3 by Zhang et al.[103] found that C_{60} was particularly inert. Small carbon clusters (C_n, with n<40) were found to be very reactive, while the larger even n clusters (40<n<80) were relatively inert. The relative inertness of the even clusters in the

40-80 range suggested that these clusters (but not the odd ones) too can form closed shells by using a combination of pentagons and hexagons. Kroto[104] has presented a set of simple, empirical chemical and geodesic rules that relate the stability of carbon cages mainly to the disposition of pentagonal rings, or various directly fused pentagonal ring configurations. He predicted that the fullerenes C_n for which n = 24, 28, 32, 36, 50, 60 and 70 should have enhanced stability relative to near neighbors.

Thompson[105] has used Euler's relations to deduce that in such a structure, there will always be 12 pentagons together with n/2 - 10 hexagons, where n is the number of carbon atoms. The most stable clusters are those with only moderately strained rings and a large number of resonance forms. C_{60} for instance has been calculated to have 12500 Kekule structures.[106]

Cox, Reichmann and Kaldor[107] have suggested that the enhanced C_{60}^+ signal observed by Smalley and coworkers could be due to an increased cross section for the formation of C_{60}^+ at the frequency of the ionizing laser and not due to its added stability. Both Smalley[103,108] and Cox[107] observed an intense peak for C_{60}^+ using F_2(7.9 eV) and ArF(6.4 eV) ionizing lasers. However, Cox and coworkers observed a greatly diminished C_{60}^+ peak using a KrF(4.99 eV) ionizing laser.

A remarkable feature of these cage structures is that they are hollow and present the possibility of trapping a wide variety of atoms inside the sphere. The concept of hollow molecules made from two-dimensional carbon sheets was first suggested by Jones[109] in 1966. He showed that Euler's closure requirement,

$$12 = 3n_3 + 2n_4 + 1n_5 + 0n_6 - 1n_7 - 2n_8 -...$$

where n_k is the number of k-sided faces, applies to such cages. For carbon only cages, k = 5 or 6 are likely (although k = 7 should not be overlooked) so 12 pentagonal faces are necessary although the number of hexagonal ones is arbitrary.

Heath et al.[110] and Weiss at al.[111] have produced stable complexes of the formula $C_{60}M$ where M = La, K and Cs by treating the graphite disks with the corresponding alkali metal halides. Cox, Reichmann and Kaldor[107] have reported attaching more than one metal atom to C_{60} and producing ions with the formulae C_nK^+, $C_nK_2^+$ and $C_nK_3^+$ for $40<n<80$.

O'Brien, Heath, Curl and Smalley[108] have generated large jet-cooled cluster ions as large as C_{80} by the direct vaporization of graphite, without the use of an ionization laser, and studied the laser-induced fragmentation behavior of these ions by tandem TOF-MS. They found that two distinct photophysical regimes could be identified. The first applied

to clusters with 34 atoms or more, all of which dissociate to produce even numbered fragments. Large even clusters fragmented by the loss of high energy C_2, while odd ones lost a single C atom. The second regime applied to clusters composed of 31 atoms or less, all of which fragment by the loss of C_3. These two regimes were separated by C_{32}^+ which fragments to produce smaller cluster ions in the 10 and 19 atom size ranges. These results were interpreted as consequences of the large even clusters having edgeless, spheroidal cage structures with the small ones having linear or ring structures.

UPS studies of mass-selected negative ion clusters by Yang et al.[112] in the 48 to 84 atom range revealed three closed shell clusters with appreciable HOMO - LUMO gaps: C_{50}(0.3-0.6 eV), C_{60}(1.5-2.0 eV) and C_{70}(0.7-1.2 eV). C_{60} was also found to have the lowest electron affinity (2.6-2.8 eV) of any cluster. Heath, Curl and Smalley[113] have observed a narrow band at 386 nm in the UV absorption spectrum of C_{60}, and assigned it to the 0-0 band of the first allowed $^1T_{1u} \leftarrow {}^1A_g$ electronic transition. The measurement was made using "laser depletion spectroscopy" based on the absorption and depletion of the C_{60}-adduct$^+$ signals, the adduct being either a C_6H_6 or CH_2Cl_2 molecule. This was in agreement with the calculations of Larsson, Volosov and Rosen[114] for the energy of the lowest electric dipole allowed transition of icosahedral C_{60}. The UPS results along with the observation

of a single narrow absorption in the UV suggested a rigid, highly symmetrical structure for C_{60}.

Very high mass even carbon clusters have been prepared by Lineman, Somayajula, Sharkey and Hercules[115] by the ionization of chrysene, pyrene and anthracene by a fourth harmonic (265 nm) Q-switched Nd-YAG laser. Positive C_n^+ cluster ions for n = 50 to 584 and negative cluster ions C_n^- up to n = 200 were observed by this method. The laser energy and focus conditions were found to play a key role in the type of carbon cluster formed. In contrast to previous studies, no dominant C_{60}^+ or C_{60}^- peak was observed in the mass spectra. This was in agreement with Cox, Reichmann, and Kaldor's[107] earlier work, where they showed that the magnitude of the C_{60}^+ signal could be influenced by the frequency of the ionizing laser and suggested that the intense C_{60}^+ signals of earlier experiments could be due to a favourable ionization cross-section at the laser frequency used, and not due to any inherent stability of the cluster. The 265 nm Nd-YAG (4.69 eV) used by Lineman et al. was very close in energy to the KrF(4.99 eV) ionizing laser used by Cox and coworkers.

O'Keefe, Ross and Baronavski[116] have also reported preparing very high mass positive carbon cluster ions C_n^+ up to n = 110 by the direct vaporization of graphite using a Nd-YAG laser. They found that this required high laser energy (>10 mJ) and long irradiation times. In contrast,

Lineman et al.[115] have produced the same clusters from chrysene using a single laser shot at relatively low laser energy (2.0 μJ; power densities less than $1x10^6$ W/cm^2).

The possible existence of such highly stable and symmetric clusters as C_{60} has provoked a great deal of interest among theoreticians.[117-130] Most of these, consisted of semi-empirical calculations extending the planar Huckel theory and including the three dimensional character of the cluster. It involved placing the pi orbitals at an angle of 23 degrees with respect to each other, and required a rehybridization of the carbon atom.

These calculations generally agreed on the stability of the truncated icosahedral structure of C_{60}. The HOMO-LUMO energy gap was found to be somewhere between 2.2 and 4.2 eV and the qualitative ordering of energy levels and bond character were in general agreement. Two ab initio calculations, the first by Disch and Schulman[131] at the STO-3G level and the second by Luthi and Almlof[132] at the large-scale restricted Hartree-Fock level have been performed yielding bond distances, the ionization potential and the electron affinity. Vibrational frequencies have been calculated by Newton and Stanton,[128] Disch and Schulman,[131] Coulombeau and Rassat,[133] Wu, Jelski and George,[134] and Weeks and Harter.[135] Due to its high symmetry, the C_{60} molecule has only four Infrared active (t_{1u}) and ten Raman active (eight h_g and two a_g) fundamentals.

Ionic Clusters

The laser vaporization of graphite is known to produce ions in addition to the dominant neutral species. Honig[6] discovered as early as 1954 that graphite filaments heated to 2600 K emitted negative carbon clusters C_n^- containing between one and eight atoms with the dominant species being C^-, C_2^- and C_3^-. Drowart *et al.*[8] measured the ionization potential of C_2 and found it to be 12.0 ± 0.6 eV. Furstnau, Hillenkamp and Nitsche[8] and Bloomfield *et al.*[136] generated positive and negative ions by the direct laser vaporization of graphite. Geusic *et al.*[137] conducted detailed studies on the photofragmentation of carbon cluster cations containing between 3 and 20 atoms. For most of the cations, the loss of C_3 was observed to be the dominant reaction channel, possibly due to the special stability of C_3. C_5^+ was observed to fragment to C_2 and C_3^+, probably due to the lower ionization energy of C_3. C_{11}^+ was another exception with the dominant channel being C_1 loss to produce C_{10}^+. Reactions of carbon cluster cations with small molecules like D_2 and O_2,[98] HCN,[99] CH_4, C_2H_2 and C_2H_4[100] by McElvany and coworkers revealed that C_7^+, C_8^+ and C_9^+ react at two different rates. This was attributed to the existence to two isomers, with the more reactive isomer assumed to be linear, while the slower reacting ions were assumed to be cyclic. An abrupt change in reactivity was also observed as the cluster

ion size increased from n = 9 to n = 10. This too was interpreted as due to a change in structure from linear to cyclic, with all clusters greater than or equal to ten atoms being cyclic.

On the theoretical front, Bernholc and Phillips[81] carried out self-consistent MNDO calculations on neutral, positive and negative chains and rings in the C_2-C_{26} range and predicted that the most stable positive ions should be C_{11}^+, C_{15}^+, C_{19}^+ and C_{23}^+ and the most stable negative ions C_{14}^-, C_{18}^- and C_{22}^-.

Very little is known about the electronic and vibrational structure of carbon cluster ions. C_2^+ was first identified by O'Keefe, Derai and Bowers,[138] and later in a neon matrix by Forney, Althaus and Maier.[139] They formed $^{12}C_2^+$ and $^{13}C_2^+$ by the photolysis of acetylene and halogenated acetylenes with the best results obtained with chloroacetylene. Three bands corresponding to the $B^4\Sigma_u^- \leftarrow X^4\Sigma_g^-$ transition were observed. The same transition was later studied by laser excitation spectroscopy by Rosslein, Wyttenbach and Maier[140] and Maier and Rosslein.[141]

The first observation of electronic transitions in C_2^- was by Herzberg and Lagerqvist,[24] who saw both absorption and emission between the ground $X^2\Sigma_g^+$ and excited $B^2\Sigma_u^+$ states in a flash discharge of methane. The carrier of those bands was identified by Lineberger and Patterson[142] by the two-photon photo-detachment spectroscopy of C_2^- in a mass-

selected negative ion beam. Subsequent work[143-146] by Lineberger's group established the electron affinity of C_2 and determined rotational and vibrational constants for the B and X electronic states. Oka and coworkers[147] have observed the infrared spectrum of the $A^2\Pi_u \leftarrow X^2\Sigma_g^+$ transition of C_2^- by using difference laser frequency spectroscopy. The ion was also prepared in argon matrices by Milligan and Jacox[148] using VUV photolysis of acetylene and using X-irradiation of acetylene in Ar, Kr and Xe matrices by Frosch.[149] The $B^2\Sigma_u^+ - X^2\Sigma_g^+$ transition was observed in both emission and absorption in all three matrices.

Carbon Clusters and Soot Formation

The kinetics of soot particle growth[1,150] has been a topic of much interest and research because of its importance in understanding combustion processes. Zhang *et al.*[103] have proposed a scheme for the formation of C_{60} as a byproduct of soot formation. Significant support for their proposal was provided by Gerhardt, Loffler and Homann[151] who reported observing C_{60}^+ as a dominant ion in a sooting flame.

Kroto and McKay[152] have proposed a carbon nucleation scheme involving a corannulene framework which results in quasi-single crystal particles of concentric, spiral-shell internal structure and overall quasi-icosahedral shape. They

have also proposed that due to the ample quantities of hydrogen present in soot, there may be no need for pentagons to form stable, more or less closed structures since stability could be acheived simply with hexagonal nets and internal C-H bonds with the hydrogens located at pentagonal vertices with respect to each other. An intriguing way to look at this surface, is as a single sheet of hexagonal graphite with 12 pentagonal defects (only 12, whatever the size) systematically inserted during growth to form an essentially continuous icosahedral monosurface. The growing onion-like particle would have a distorted icosahedral shape. This proposal received substantial support when Iijima[153] observed polyhedral concentric shell structures in electron micrographs of carbon particles.

It is clear that the chemistry of carbon clusters is rich and varied, and many questions about the structures, and the electronic and vibrational properties of even the smaller clusters remain to be answered. The practical implications of a thorough knowledge of carbon cluster chemistry could be profound in areas ranging from combustion and catalysis to the mechanism of thin film growth and interstellar chemistry. This thesis deals with the characterization of some small carbon clusters by infrared spectroscopy. Specifically, it presents evidence for the vibrational frequency assignments and ground state geometries of C_5, C_6, C_8 and C_5^+.

CHAPTER II

EXPERIMENTAL

A detailed description of the experimental setup used to generate and study the carbon clusters is presented here. Matrix isolation involves mixing the vapour of the sample of interest with a large excess of the matrix gas (typically an inert gas) and freezing the mixture on a cold window to form a matrix. The sample molecules are trapped in the solid inert gas and isolated from each other. This minimizes or eliminates interactions between the sample molecules and greatly simplifies spectra. Also the molecules are vibrationally cold at the temperatures used. Matrix isolation spectrosopy offers an ideal technique to study highly reactive species such as radicals and ions. The matrix allows one to stabilize and accumulate these species in sufficiently high concentrations to allow study by absorption spectroscopy.

Experimental Approach

The approach used in this study to identify the sizes and ground state geometries of the clusters identified is a variant of the well-known isotopic substitution method in infrared spectroscopy. The method involves, first, the infrared spectral recording of the products of vaporized ^{12}C graphite, followed by the recording of the products of a vaporized sample from a 1:1 mixture of ^{12}C:^{13}C graphite powder. For a particular cluster size and geometry, all the isotopomeric structures possible can be expected if, during the laser vaporization process, the graphitic carbon is atomized and the atoms react to form clusters before deposition in the matrix.

The number of isotopomers formed for any given cluster is dependent on the geometry of the cluster. Thus, the number of different isotopomeric infrared frequencies observed in the 1:1 mixture run, is direct information on the geometry and size of the cluster. Generally, the number of isotopomeric bands does not lead to a unique choice of cluster size and geometry, but the choices are considerably narrowed. In order to collapse these choices to a final one, a normal coordinate analysis is performed. A good fit is effected when the deviation of the observed and predicted bands is small and the force constants used to obtain the fit are reasonable.

To illustrate the method, the C_3 cluster will be discussed. Three structures are possible: linear, bent and cyclic (equilateral triangle). Figure 2.1 shows the number and types of isotopomeric structures expected for the linear and cyclic cases. The shaded circles represent ^{13}C atoms. The bent case is similar to the linear structure and will have an identical number of isotopomers as the linear case, the only difference being the angle subtended by the two external carbons on the central carbon atom. It can be seen that the linear and bent structures possess six isotopomers while the cyclic structure has only four isotopomers.

C_3 has one infrared active stretching vibration with σ_u^+ symmetry. The value of this vibrational frequency for the ^{13}C substituted isotopomers will be red shifted relative to the $^{12}C_3$ frequency by varying amounts, with the all-$^{13}C_3$ isotopic frequency being red shifted the most. For linear carbon clusters, it can be shown from the Teller-Redlich rule[154] that the frequencies for the two completely substituted isotopomers will obey the relation

$$^{13}\nu_i \; / \; ^{12}\nu_i = 0.9606.$$

This relation dictates that for ^{12}C cluster frequencies in the 2000 cm^{-1} (C-C stretch) range, its ^{13}C partner will absorb ~80 cm^{-1} to lower energy. The mixed isotopomers will, of course, fall within these limits.

Figure 2.1

Isotopomers of C_3.

(a) linear structure.
(b) cyclic structure.

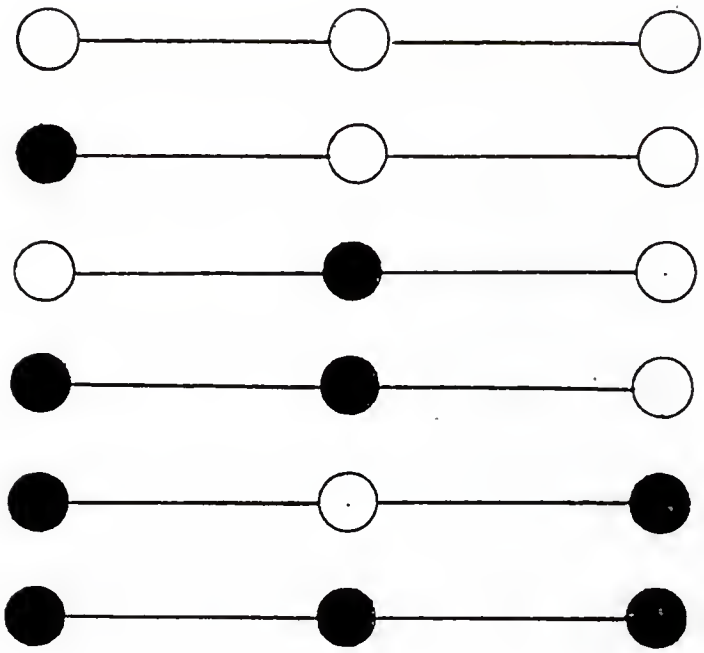

(a)

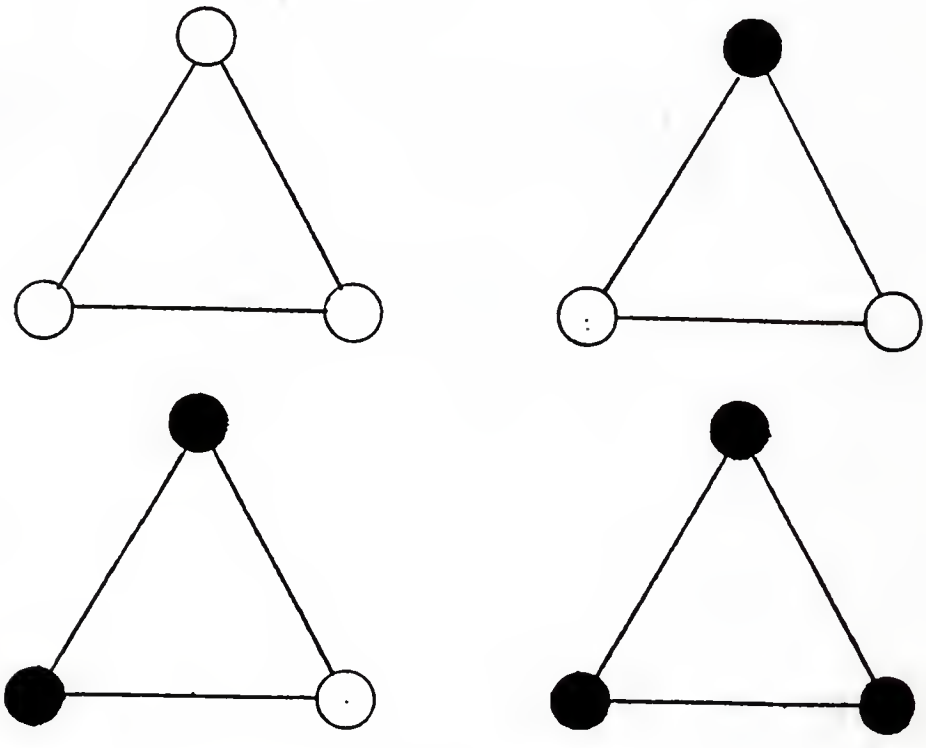

(b)

Figure 2.2 shows the infrared spectrum of the products of laser vaporized graphite in an argon matrix (200 scans, 0.25 cm^{-1} resolution). The bottom panel shows the spectrum of ^{12}C in argon while the top one shows the spectrum for the 1:1 mixture of ^{12}C and ^{13}C isotopes. Both spectra are for unannealed matrices. It can be seen that six bands are built on the 2039 cm^{-1} band with the lowest energy band appearing at 1961 cm^{-1} or 78 cm^{-1} away from the all-^{12}C isotopomer band at 2039 cm^{-1}. The appearance of six bands conclusively excludes the equilateral cyclic structure but does not allow a distinction between the bent or linear structures. However, the spread of the six bands fulfills the Teller-Redlich criterion for linear molecules.

To confirm this conclusion, a normal coordinate calculation can be carried out and the predicted bands fit to the experimentally observed ones. A good fit with reasonable force constants would constitute conclusive proof for the above assignment. Weltner and McLeod[17a] have obtained such a fit and determined the force constants to be 10.34 mdyn/Å (for the C-C stretch) and +0.542 mdyn/Å for the interaction between the adjacent C-C stretches.

An similar approach has been used to assign the vibrational frequencies and determine the structures of the C_5, C_6, C_8 and C_5^+ clusters, the subjects of this study.

Figure 2.2

Infrared spectrum in the 2070-1930 cm^{-1} region of laser-ablated ^{12}C products (lower spectrum) and ^{12}C:^{13}C isotopically-mixed products (upper spectrum) in unannealed argon matrices at 12 K showing the six C_3 isotopomeric bands. Resolution = 0.25 cm^{-1}.

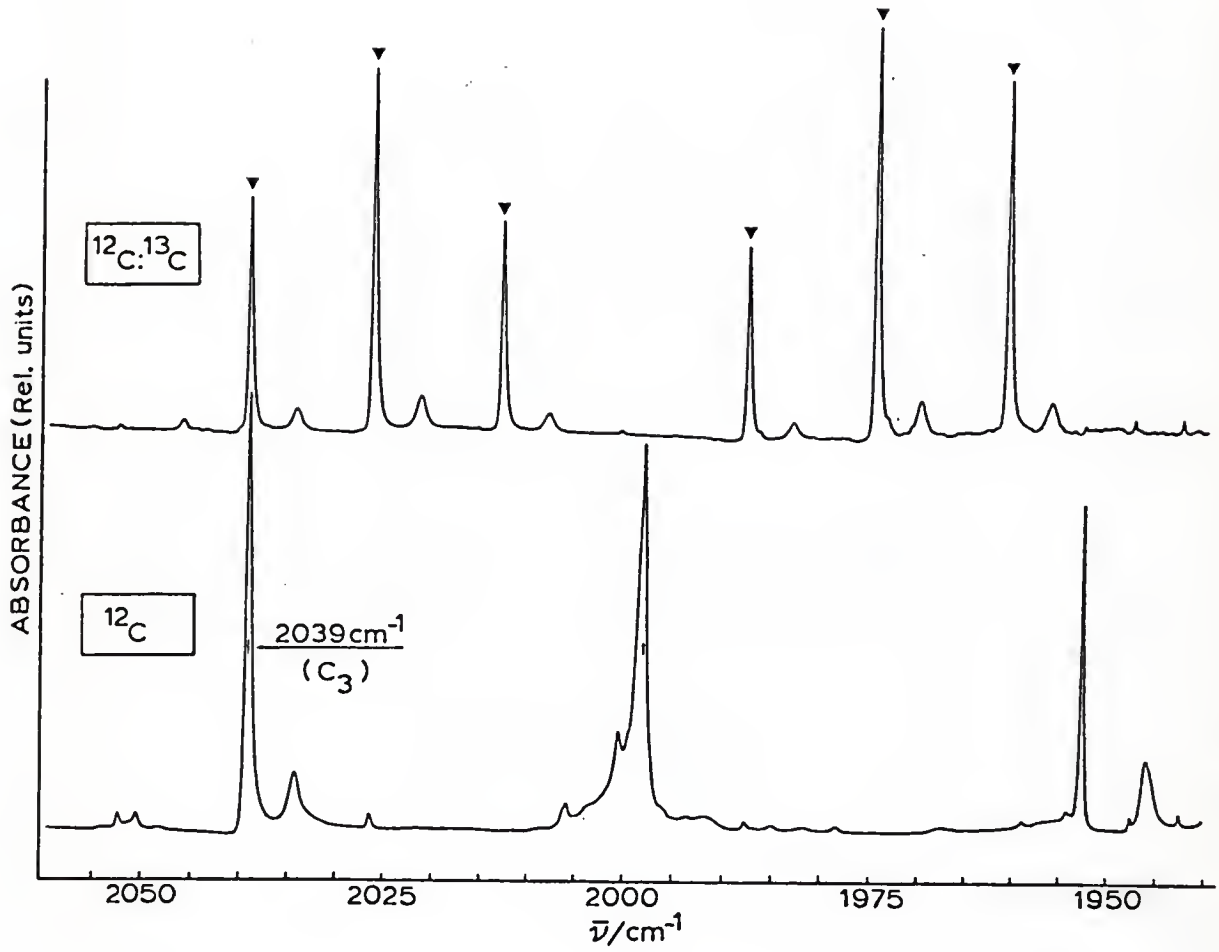
$^{12}C:^{13}C$
^{12}C
2039 cm^{-1}
(C_3)
ABSORBANCE (Rel. units)
2050
2025
2000
1975
1950
$\bar{\nu}$/cm^{-1}

Matrix Isolation Apparatus

The apparatus used to achieve the temperatures necessary for the formation of inert gas matrices consisted of a two stage helium refrigerator (Air Products, Displex Model DE202), shown in Figure 2.3. A Knudsen cell furnace assembly is shown attached to the shroud. Cooling is achieved by the expansion of compressed helium gas. Temperatures as low as 10K can be reached. The cold window assembly was mounted on a cold finger at the bottom of the second stage and was surrounded by a copper radiation shield attached to the first stage of the Displex. The radiation shield, maintained at 40-60 K, acted as a thermal barrier to heat transfer from the outer vacuum shroud to the lower stage and the window assembly. The cryostat could rotate ninety degrees in either direction inside its fixed outer vacuum shroud. Figure 2.4 shows the the details of the Knudsen cell furnace assembly and the Knudsen cell. The setup shown was used to degas the sample of ^{13}C before use in the experiment.

The temperature of the sample window was set by an Air Products APD-B temperature controller and measured by a gold-chromel, 0.07% Fe thermocouple with the thermocouple junction mounted near the middle of the oxygen free copper window holder. The thermocouple was calibrated against the temperature of liquid nitrogen. The cold finger was equipped

Figure 2.3

Cryostat and furnace assembly.

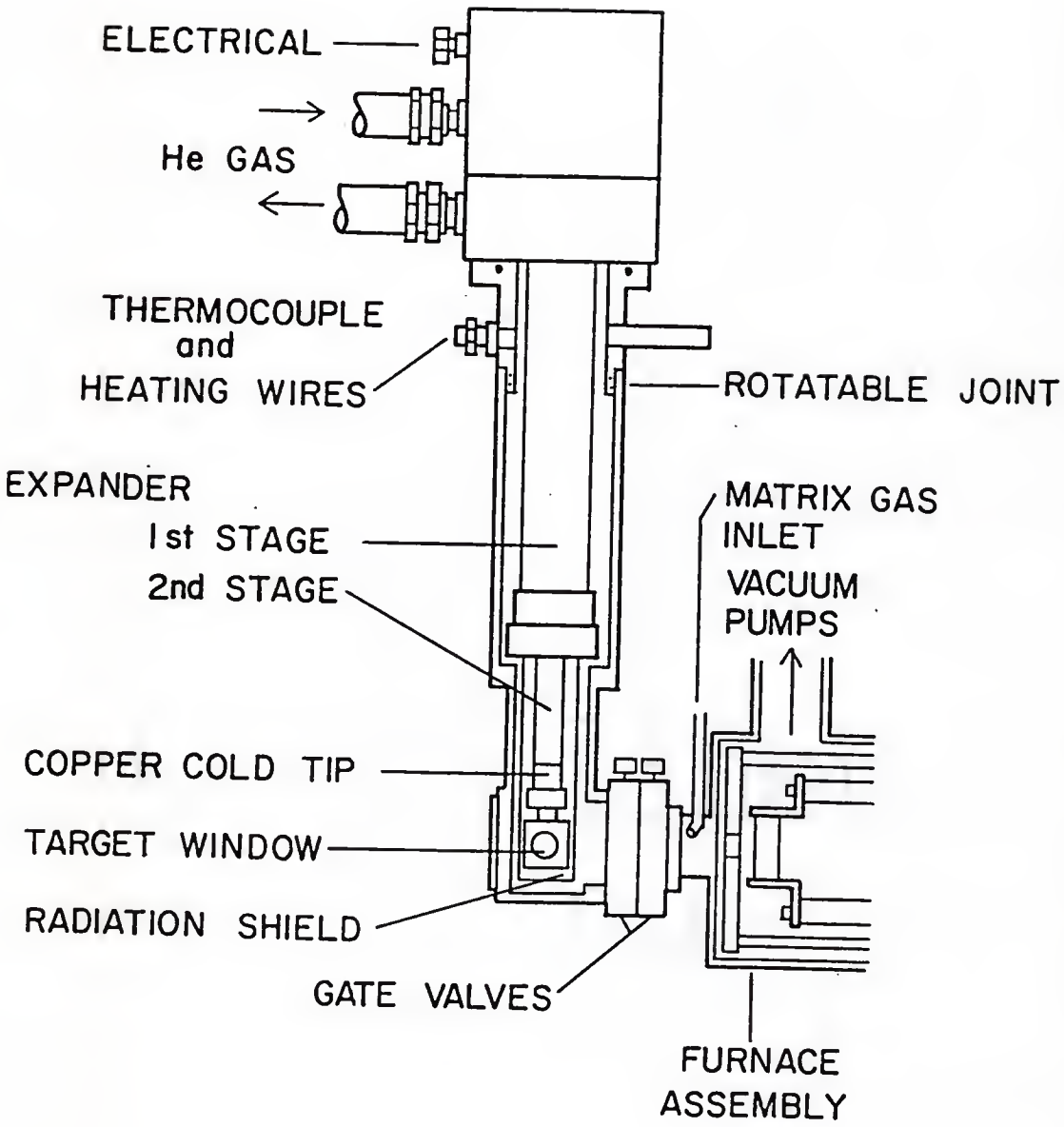
ELECTRICAL
He GAS
THERMOCOUPLE
and
HEATING WIRES
ROTATABLE JOINT
EXPANDER
1st STAGE
2nd STAGE
MATRIX GAS
INLET
VACUUM
PUMPS
COPPER COLD TIP
TARGET WINDOW
RADIATION SHIELD
GATE VALVES
FURNACE
ASSEMBLY

Figure 2.4

Sample Degassing Setup.

(a) Furnace assembly.
(b) Knudsen Cell.

(a)

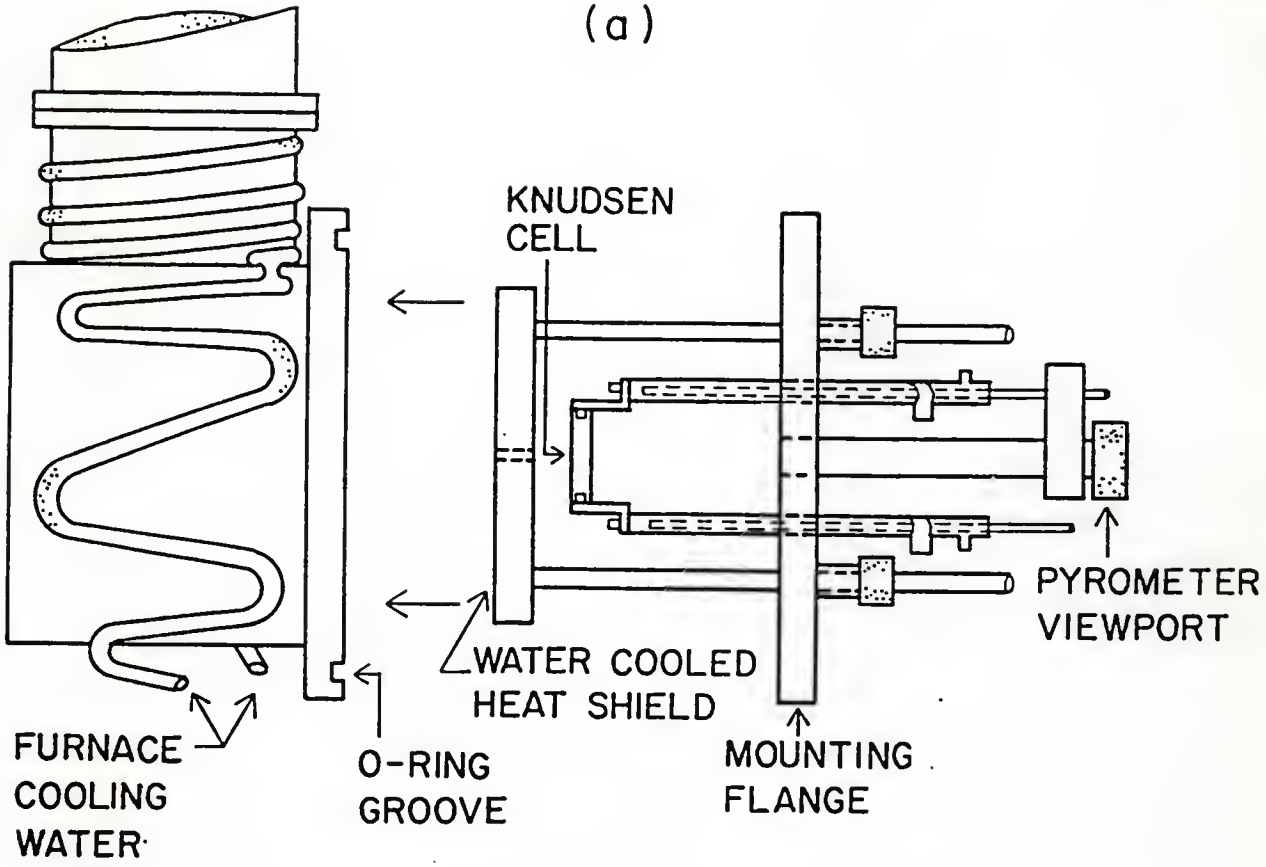
KNUDSEN
CELL
PYROMETER
VIEWPORT
WATER COOLED
HEAT SHIELD
FURNACE
COOLING
WATER
O-RING
GROOVE
MOUNTING
FLANGE

(b)

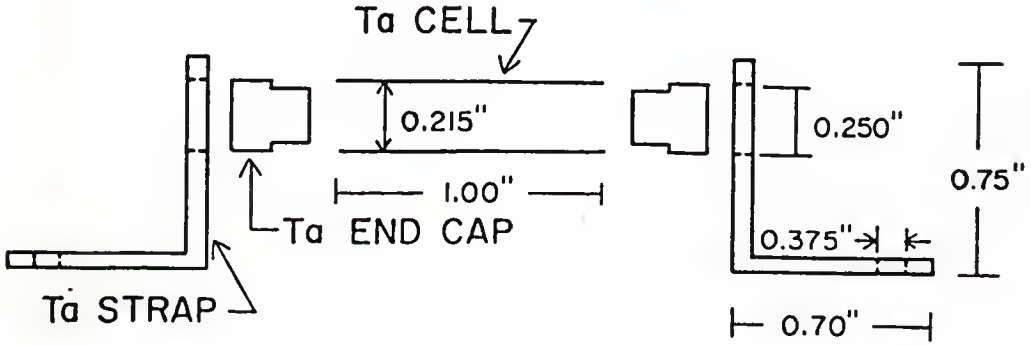
Ta CELL
0.215"
1.00"
Ta END CAP
Ta STRAP
0.250"
0.75"
0.375"
0.70"

with a 10 watt variable duty cycle heater used to control the temperature of the window. The window assembly was screwed on to the cold-finger of the cryostat and an indium gasket was used to ensure good thermal contact with the cold-finger.

The interior of the shroud was evacuated to pressures less than 1 X 10^{-6} Torr. by a two inch air-cooled oil diffusion pump (Alcatel PDR 250, pumping speed = 200 L/sec.) and a 450 L/minute mechanical roughing pump (Alcatel 2020). The low pressures are necessary to achieve the low temperatures and to prevent the condensation of contaminants including atmospheric gases on the window. The pressure was monitored by an ion gauge (Model 4336P, Kurt J. Lesker Co.) and read off a Granville-Phillips 270 Gauge Controller.

Carbon Cluster Preparation

The carbon clusters were generated by focussing the second harmonic output (532 nm, ~0.1 mJ/pulse, 10 Hz) of a pulsed Q-switched Nd-YAG laser (Spectra Physics, DCR-11 Nd-YAG) on the graphite rod. The rod was rotated at a rate of approximately 6 rev./hr. to expose a fresh surface for every pulse. The graphite vapour that resulted was mixed with argon gas and deposited on the cryostat's cesium iodide window which was maintained at 12 K. The high purity argon gas (Research purity, 99.9995% pure, Matheson Gas Products)

was bled into the cryostat through a micro-metering needle valve (Whitey Co.) in a continuous flow. Factors that influence the production of a good matrix include laser power, laser focus, the distance between the carbon source and the sample deposition window, and the flow rate of the matrix gas. These factors had to be varied and optimized to get the spectra described in this work.

For the mixed isotope experiments, a 1:1 mixture of ^{12}C and ^{13}C powders was pressed into a pellet and mounted on the side of the Displex shroud as shown in Figure 2.5. The ^{12}C powder was prepared by scraping a rod of the afore-mentioned graphite. The ^{13}C powder (98.4 atom%, Isotec Inc.) was degassed in a tantalum Knudsen cell at 1500 K for one hour before mixing with the ^{12}C powder. The laser was focussed on a different spot on the pellet every 5 minutes during deposition.

In order to distinguish between ions and neutrals, a modification to the experimental setup described above was necessary. A small copper wire ring was mounted ~0.5 cm in front of the sample window and electrically insulated from it and its copper mount. This was done by tying the copper ring to two parallel glass capillary tubes and gluing the glass tubes to the copper window mount as shown in Figure 2.6. By applying a potential to the ring ions could either be attracted to or repelled from the deposition window depending on the polarity of the ring with respect to the

Figure 2.5

Experimental setup for the matrix isolation of laser-ablated carbon in argon.

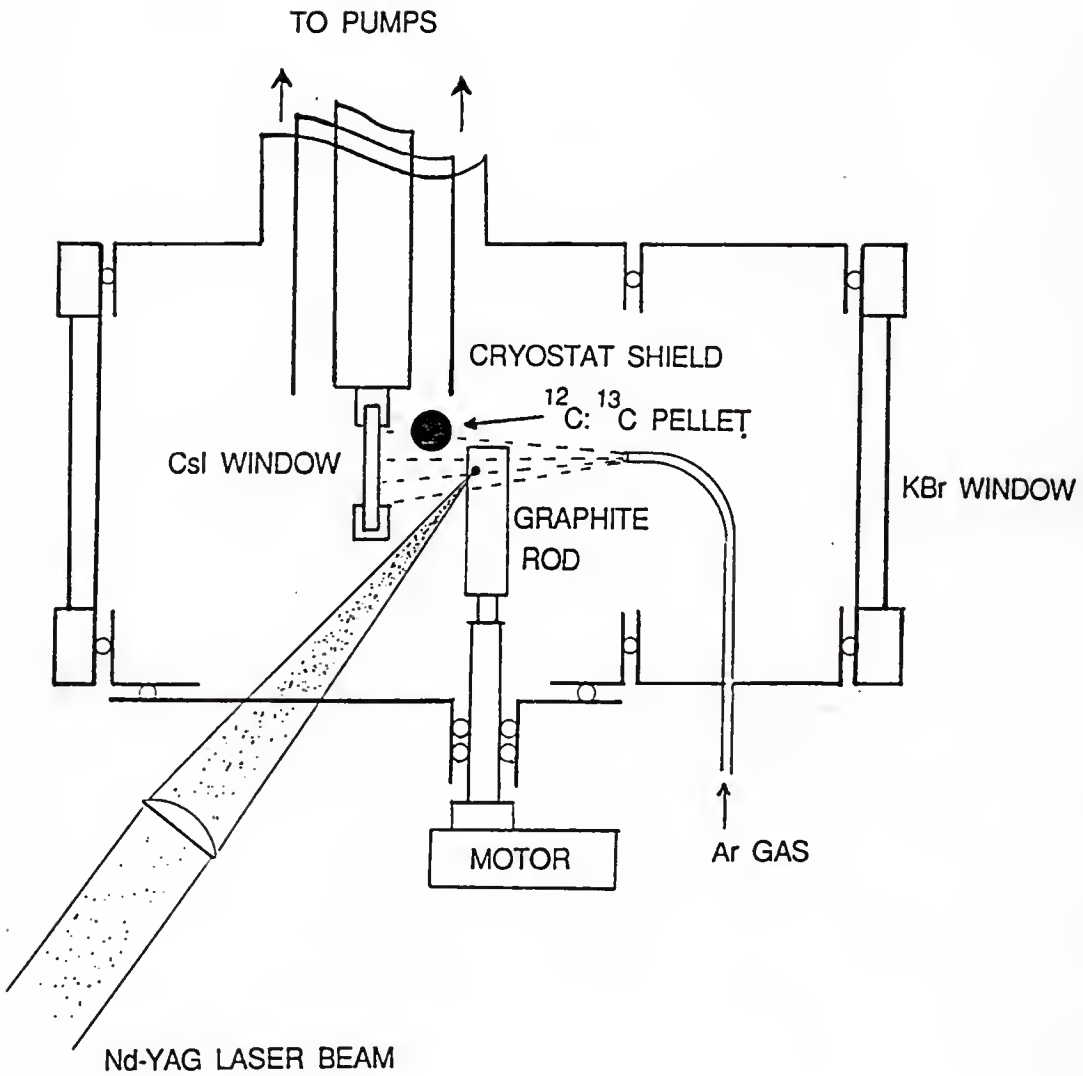
TO PUMPS
CRYOSTAT SHIELD
^{12}C: ^{13}C PELLET
CsI WINDOW
KBr WINDOW
GRAPHITE
ROD
MOTOR
Ar GAS
Nd-YAG LASER BEAM

Figure 2.6

Experimental setup for distinguishing between ions and neutrals in the argon matrix.

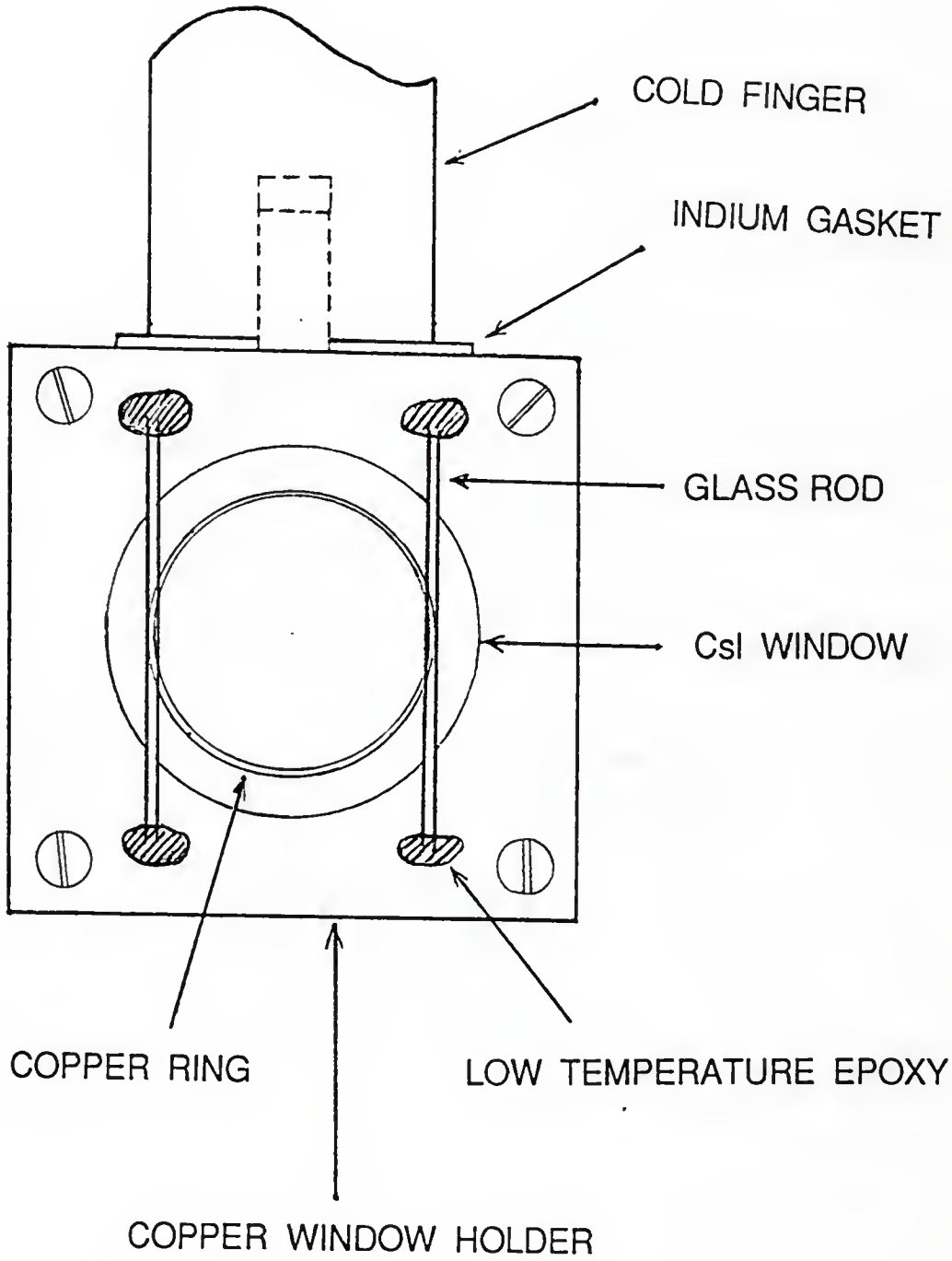
COLD FINGER
INDIUM GASKET
GLASS ROD
CsI WINDOW
COPPER RING
LOW TEMPERATURE EPOXY
COPPER WINDOW HOLDER

window holder which was held at ground. In a second approach, a small tungsten filament acting as an electron gun was mounted in close proximity to the sample window (~2.0 cm), and used to neutralize any positive ions present in the matrix. Simultaneously, a band at 904 cm^{-1}, ascribed to the ArH^+ ion[155] was also monitored for changes in its intensity.

Instrumentation

A Nicolet 7199 Fourier Transform Infrared spectrometer was used to record the infrared data. It was equipped with a water cooled globar source and MCT and TGS detectors. All the spectra used in this work were recorded by the MCT detector due to its greater sensitivity and better signal-to-noise ratio. The spectrometer was purged with dry nitrogen to exclude any water in the optical path and to protect the beam splitter.

The heart of the spectrometer consists of a Michelson interferometer. One arm of the interferometer has a stationary plane mirror while the other arm has a movable mirror assembly mounted on dual air bearings and driven by a linear induction motor. Light from the source is split by the KBr beamsplitter and travels down the two arms of the interferometer to be reflected back to the beam splitter and through the sample on to the detector. The recombined beam

leaving the beamsplitter shows constructive or destructive interference, depending on the relative path lengths from the beamsplitter to the fixed mirror and the beamsplitter to the moving mirror assembly. If the path lengths are identical or differ by an integral number of wavelengths, constructive interference occurs, whereas if the difference is a half-integral number of wavelengths, the beams cancel at the beamsplitter. By moving the moving-mirror assembly, the flux at the detector is varied and one obtains an interferogram. Each data point on the interferogram is the sum of individual frequencies. The frequency domain data of interest is then recovered by performing the Fourier Transform on the interferogram. This operation is performed by the Nicolet 1180 computer.

Fourier Transform spectroscopy allows one to detect very weak signals with relatively high signal-to-noise ratio by just increasing the number of scans collected. This is of importance in the experiments of interest, since many of the clusters (especially in the mixed isotope experiments) are present in very small concentrations.

CHAPTER III

THE C_5 CLUSTER

Introduction

The first calculation on C_5 was conducted Pitzer and Clementi[67] and predicted a linear structure for the molecule. Ewing and Pfeiffer[82] have calculated the total energies, bond lengths, charge distribution and electronic configurations for linear C_n clusters for n = 2-6. Later calculations[83,84] by them took a number of non-linear geometries into account as well and found the linear singlet form to be the most stable by more than 60 kcal/mole. Similar conclusions were reached by Ott and Ray[85] in a recent study on equilibrium geometries of C_n clusters. A MINDO/2 study by Slanina and Zharadnik[156] predicted the most stable structure of C_5 to be a trigonal bipyramid.

An infrared study of matrix isolated carbon clusters has been performed by Thompson, DeKock and Weltner.[86] In this work carbon was vaporized from a tantalum furnace (yielding C, C_2 and C_3) and the larger clusters were produced by annealing the matrix. Infrared bands were

correlated by their intensity behaviour upon annealing and structures assigned from partial isotopic studies using 95%-enriched ^{13}C in conjunction with normal coordinate calculations. The 1952 cm^{-1} and 1544 cm^{-1} bands were assigned to the σ_u stretches of $^{12}C_5$.

In the present investigation a similar approach was adopted. First, those bands that correlated with each other in terms of change in intensity upon annealing were identified. Second, the mixed isotope effect (1:1 mixtures of ^{12}C:^{13}C) was used to assign a particular IR band to a specific carbon cluster and to determine the cluster geometry. This was done by comparing the number of isotopomeric structures expected for a certain geometry with the number of isotopomeric peaks observed. The assignment was then confirmed by performing a normal coordinate analysis on the molecule and fitting the calculated frequencies to the observed ones. The resulting force constants were found to be reasonable, and provided evidence for the assignment of the 2164 cm^{-1} band to linear C_5.

Results

The infrared spectrum of the ^{12}C products obtained via laser ablation of graphite is similar to that obtained by thermal vaporization followed by strong annealing. Figure

3.1 shows the prominent bands observed here, (2164 cm^{-1}, 2039 cm^{-1}, 1998 cm^{-1} and 1952 cm^{-1}) which have been seen previously by Thompson, DeKock and Weltner.[86]

Isotopic substitution is a powerful method for elucidating the structures of small carbon clusters. Using a 1:1 mixture of ^{12}C:^{13}C powder, all the isotopomeric structures possible for a particular cluster geometry can be expected if, during the laser vaporization process, the carbon is atomized and the atoms react to form clusters in the vapour before deposition. Each isotopomer will give rise to an IR band whose frequency is shifted from its parent (containing only ^{12}C).

For a 1:1 sample mixture of ^{12}C:^{13}C graphite, the number of isotopomers for a particular cluster size can be easily determined. For linear clusters with even (2n) or odd (2n + 1) atoms, the number of isotopomeric species is given by

$$I_{2n} = 2(2I_{2n-2} - 2^{n-2})$$

and

$$I_{2n+1} = 2I_{2n}$$

where obviously $I_1 = 2$ and $I_2 = 3$. The possible number of isotopomers[156] is 6 for C_3, 10 for C_4, 20 for C_5 and 36 for C_6. Other possible structures for C_5 are trigonal bipyramidal, square pyramidal and cyclic, for which the

Figure 3.1

Infrared spectrum of the products of laser-ablated ^{12}C in an unannealed argon matrix. Resolution = 1 cm^{-1}.

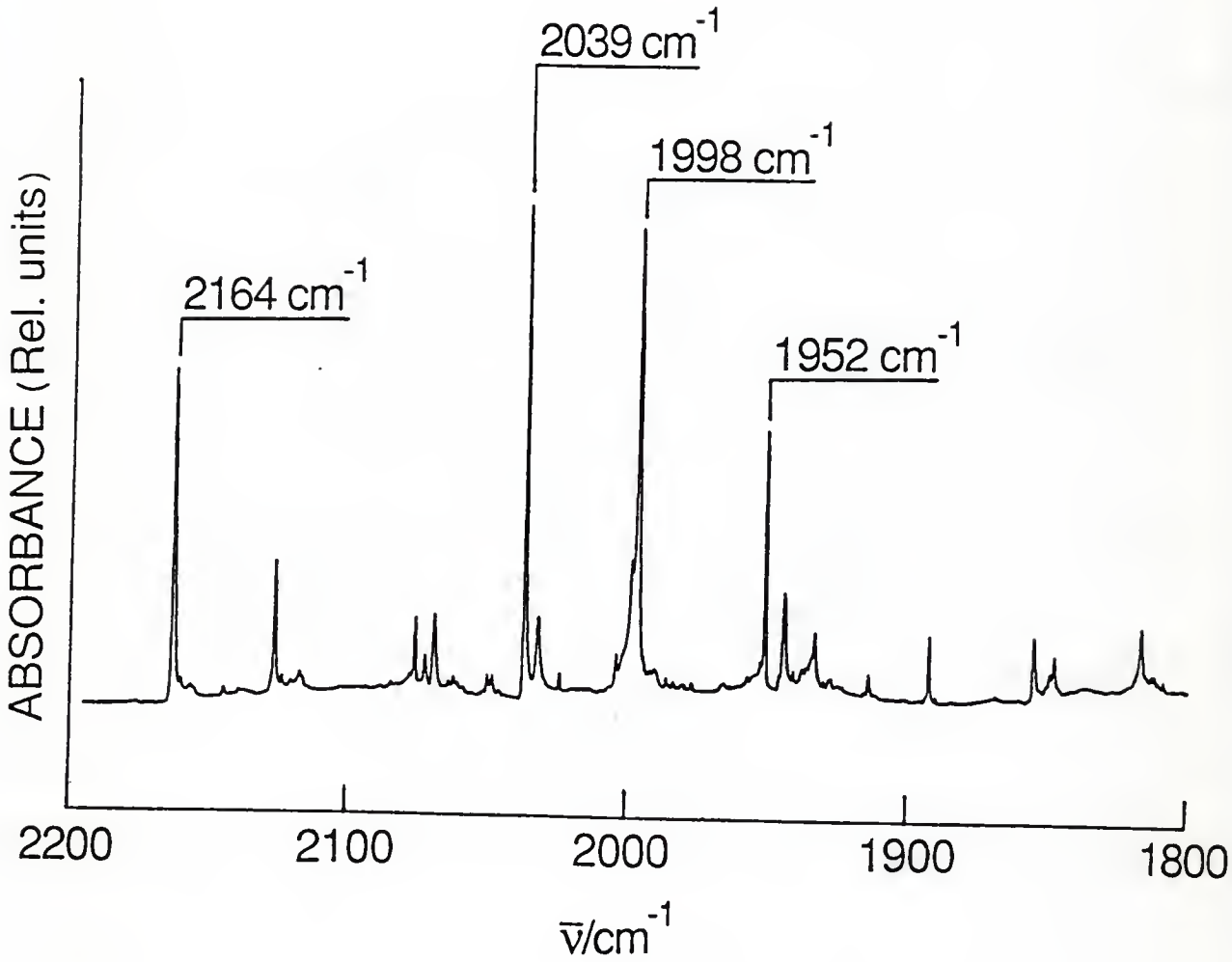
2039 cm-1
1998 cm-1
2164 cm-1
1952 cm-1
ABSORBANCE (Rel. units)
2200
2100
2000
1900
1800
ν̄/cm-1

number of isotopomers are reduced to 12, 12 and 8, respectively.

Figure 3.2 shows the infrared spectrum of the products of laser-vaporized graphite in an argon matrix (200 scans, 1 cm^{-1} resolution). The bottom panel shows the spectrum of ^{12}C in argon. It clearly shows a prominent band at 2164 cm^{-1} and a less intense band at 2128 cm^{-1}. The 2128 cm^{-1} band had previously been assigned to C_9 by Thompson et al.[86] The top panel shows the mixed isotope spectrum and clearly shows 20 bands (marked by dots) built on the 2164 cm^{-1} band. These isotopomer bands are also seen to fulfill the Teller-Redlich criterion: the separation between the bands at the extremities is 84.5 cm^{-1}. The presence of 20 isotopomer bands coupled with the fulfilment of the Teller-Redlich criterion strongly suggests that the 2164 cm^{-1} band is due to linear C_5.

Linear C_5 has two σ_u IR-active stretching vibrations, of which the the larger one is expected in the 2000 cm^{-1} region. The second band is expected to lie at lower energy. A band at 1544 cm^{-1}, about 50 times less intense than the 2164 cm^{-1} band, was observed to decrease in intensity markedly and in parallel with the 2164 cm^{-1} band upon annealing at 35 K. A search for 20 isotopomer bands associated with the 1544 cm^{-1} band was made in the mixed isotope spectrum, but none were found.

Figure 3.2

Infrared spectra of the 2180-2070 cm^{-1} region of laser vaporized graphite in an argon matrix (12 K). Top panel: 1:1 mixture of ^{12}C:^{13}C; black dots indicate bands due to isotopomers of linear C_5 (cf. Table 1); indicated 2164 cm^{-1} band is from $^{12}C_5$ and 2079.5 cm^{-1} band from $^{13}C_5$. Bottom panel: pure ^{12}C graphite; 2128 cm^{-1} band has been ascribed to $^{12}C_9$. Resolution = 1 cm^{-1}.

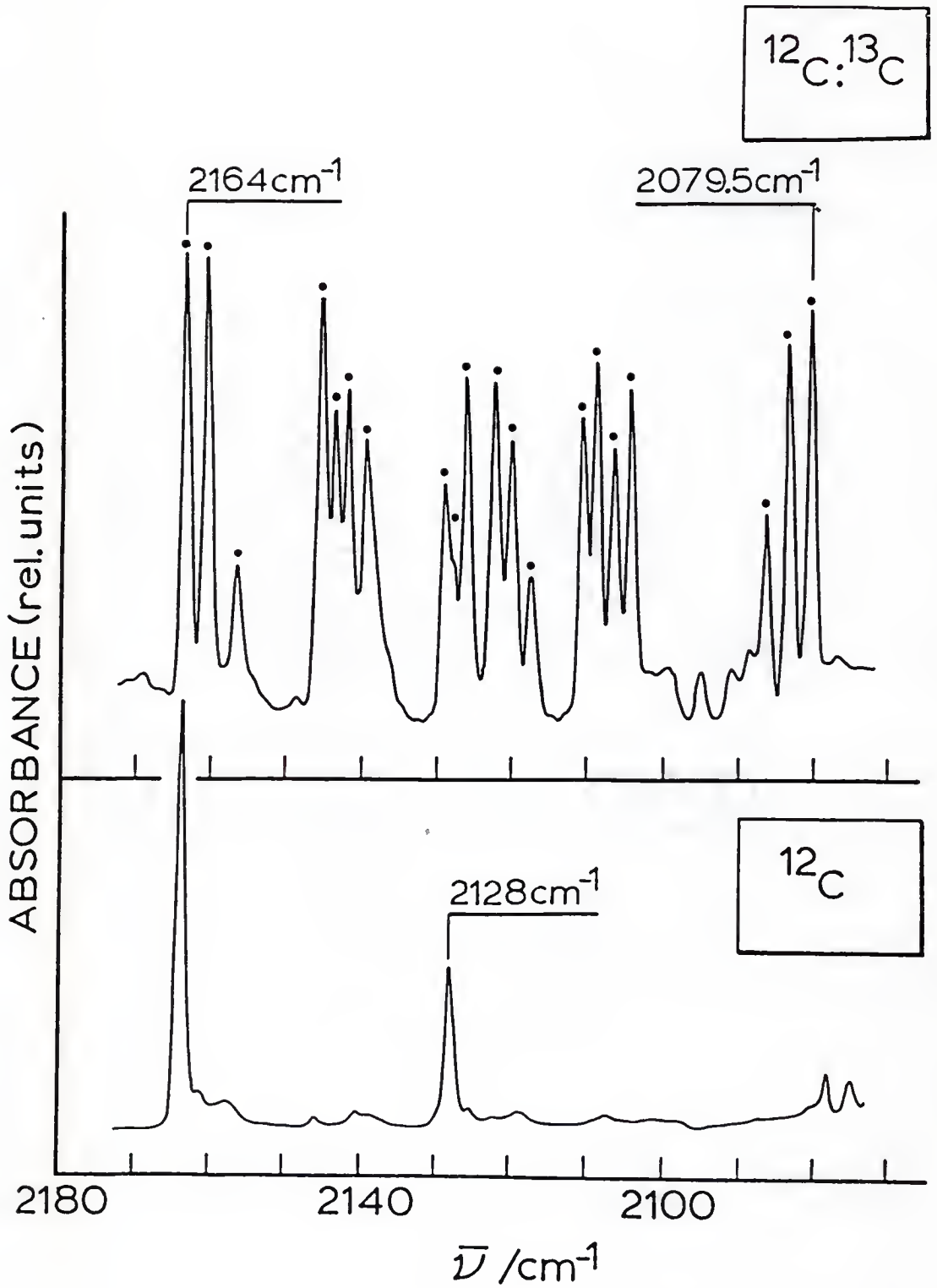
$^{12}C:^{13}C$
2164cm^{-1}
2079.5cm^{-1}
ABSORBANCE (rel. units)
^{12}C
2128cm^{-1}
2180
2140
2100
$\bar{\nu}$ /cm^{-1}

Normal Coordinate Analysis

The linear C_5 molecule possesses $D_{\infty h}$ symmetry. The σ_u asymmetric stretch is expected to be the most intense IR active band. The internal coordinates used in the calculations were 'R', the outer C-C stretch, and 'r', the inner C-C stretch. The symmetry coordinates were constructed by taking symmetry adapted linear combinations of the internal coordinates.

The symmetry coordinates[158] were defined as follows:

$S_1 = R_1 + R_2$ ------ σ_g symmetric stretch.

$S_2 = R_1 - R_2$ ------ σ_u asymmetric stretch.

$S_3 = r_1 + r_2$ ------ σ_g symmetric stretch.

$S_4 = r_1 - r_2$ ------ σ_u asymmetric stretch.

Only the C-C stretching vibrations were considered in the analysis since the bending modes were outside the range of our spectrometer. The normal coordinates obtained consisted of two σ_u IR active stretches and two σ_g IR inactive stretches. The force constants used in the analysis were designated as "f_R" for the outer bond; "$f_r - f_{rr}$" for the inner bond; "f_{RR}" for the interaction between the outer bonds and "f_{rR}" for the interaction between the outer and inner bonds. f_{RR} was assumed to be negligible and set equal to zero. In the valence force field treatment[31] of this

molecule, the terms f_{rr} and f_r always appear together in the form $f_r - f_{rr}$ and therefore no attempt was made to separate the two variables. The general expression for Σ_u^+ vibrations as given by Smith and Leroi for C_3O_2,[159] was used to calculate the values of the force constants f_R and $f_r - f_{rr}$ as a function of f_{rR}. For a symmetric carbon chain it reduces to

$$\lambda^2 - \lambda\mu_C[2f_R + 3f_r - 2f_{Rr}] + 5\mu_C^2[f_Rf_r - f_{Rr}^2] = 0 \qquad (1)$$

where $\lambda = (2\pi c\nu)^2$ and $\mu_C = 1/12$. Solving for λ, one gets

$$(\lambda_1 + \lambda_2)/\mu_C = 2f_R + 3f_r - 2f_{Rr} \qquad (2)$$

and

$$\lambda_1\lambda_2 = 5\mu_C^2[f_Rf_r - f_{Rr}^2] \qquad (3)$$

from which one obtains

$$f_r - f_{rr} = 1/6(A + 2f_{rR}) + 1/2[(2f_{rR}/3 + A/3)^2 - 8/3(B + f_{rR}^2)]^{1/2} \qquad (4)$$

and

$$f_R = (B + f_{rR}^2) / (f_r - f_{rr}) \qquad (5)$$

A and B are constants, which are defined as

$A = (\lambda_1 + \lambda_2) / \mu_C$ and $B = \lambda_1\lambda_2 / 5\mu_C^2$

The values of the force constants obtained were in millidynes per Angstrom. The previously mentioned IR bands at 2164 and 1544 cm^{-1} (ν_1 and ν_2), which were observed to behave in a parallel manner upon annealing, were used in the fit. The force constants, f_R and $f_r - f_{rr}$ vary as a function of f_{Rr}, and their values were calculated for a series of values of f_{Rr}. Sets of these three force constants for any given value of f_{Rr} were used in the normal coordinate analysis and this procedure repeated with several sets until a suitable fit was obtained. The force constants obtained by this procedure were f_r = 11.357 mdyn/Å; $f_r - f_{rr}$ = 9.989 mdyn/Å; f_{rR} = 1.350 mdyn/Å and f_{RR} = 0. Table 1 gives the list of frequencies obtained for all twenty isotopomers of C_5.

The vibrational frequencies of the linear C_5 molecule were later calculated using a different program[160] which allowed all three force constants to be varied independently and used a least squares fitting subroutine to fit the calculated frequencies with the experimental ones. The force constants obtained by this fit were comparable to the ones obtained by the earlier method. The frequencies obtained are listed in Table 2. The fit can be seen to be excellent with the rms difference between calculated and experimental frequencies equal to 1.043 cm^{-1}. The force constants

obtained were f_R = 11.109 mdyn/Å, f_r = 10.253 mdyn/Å and f_{Rr} = 1.499 mdyn/Å.

Discussion

The results of the normal coordinate analysis are presented in Table 1. The force constants obtained: f_R = 11.357 mdyn/Å , $f_r - f_{rr}$ = 9.989 mdyn/Å and f_{Rr} = 1.350 mdyn/Å, compare favourably with the force constants obtained by Smith and Leroi[159] for C_3O_2. The values of the above three force constants for C_3O_2 are 15.41, 9.34 and 1.27 mdyn/Å respectively. The excellent fit, and the reasonable values of the force constants obtained, constitute conclusive proof for the assignment of the 2164 cm^{-1} band to $^{12}C_5$.

The absence of 20 isotopomeric bands associated with the 1544 cm^{-1} band in the mixed isotope spectrum, is not surprising, given the very low intensity of the 1544 cm^{-1} band in the ^{12}C spectrum. The intensity of the isotopomeric bands, if observed, would on an average be 1/20 of the parent peak's intensity in the ^{12}C spectrum. The 1544 cm^{-1} band lacks the isotopomeric data to support its assignment with the same degree of certainty as the 2164 cm^{-1} band. This makes its assignment to linear C_5 less certain.

Recent calculations by Martin, Francois and Gibels[73] assigned the 1544 cm^{-1} band to the $^3\Sigma_g^-$ vibration of C_4 but

TABLE 1

Isotopomer Stretching Frequencies for Linear C_5.

Obs. Freq. ν/cm^{-1}	Calc. Freq.[a] ν/cm^{-1}	Difference $\Delta\nu/cm^{-1}$	Structure of Isotopomer	Stat. Wts.
2164	2164.4	0.4	12-12-12-12-12	1
2161	2161.5	0.5	13-12-12-12-12	2
2158	2158.3	0.3	13-12-12-12-13	1
2146	2144.5	1.5	12-13-12-12-12	2
2144	2142.5	1.5	12-12 12-13-13	2
2142	2140.7	1.3	13-12-12-13-12	2
2140	2138.5	1.5	13-13-12-12-13	2
2129	2132.0	3.0	12-12-13-12-12	1
2128	2128.5	0.5	13-12-13-12-12	2
2126	2124.7	1.3	13-12-13-12-13	1
2122	2120.7	1.3	12-13-12-13-12	1
2120	2117.9	2.1	13-13-12-13-12	2
2117.5	2115.0	2.5	13-13-12-13-13	1
2111	2111.6	0.6	12-13-13-12-12	2
2109	2109.3	0.3	13-13-13-12-12	2
2106.5	2106.9	0.4	13-12-13-13-12	2
2104.5	2104.4	0.1	13-13-13-12-13	2
2086	2086.5	0.5	12-13-13-13-12	1
2083	2083.1	0.1	13-13-13-13-12	2
2079.5	2079.5	0.0	13-13-13-13-13	1

[a]Force constants used: f_R = 11.357 mdyn/Å, f_r-f_{rr} = 9.989 mdyn/Å, f_{Rr} = 1.350 mdyn/Å and f_{RR} = 0. The frequencies 2164 cm^{-1} and 1544 cm^{-1} were used to determine f_R and f_r-f_{rr} while varying f_{Rr}.

TABLE 2

Observed and Calculated Isotopomer Stretching Frequencies for Linear C_5.

Obs. Freq. (ν/cm^{-1})	Calc. Freq.[a] (ν/cm^{-1})	Difference ($\Delta\nu$/cm^{-1})	Structure of Isotopomer	Stat. Wts.
2164	2164.59	-0.59	12-12-12-12-12	1
2161	2162.19	-1.19	13-12-12-12-12	2
2158	2159.69	-1.69	13-12-12-12-13	1
2146	2145.18	0.82	12-13-12-12-12	2
2144	2143.54	0.46	12-12 12-13-13	2
2142	2142.13	-0.13	13-12-12-13-12	2
2140	2140.41	-0.41	13-13-12-12-13	2
2129	2129.46	-0.46	12-12-13-12-12	1
2128	2126.55	1.45	13-12-13-12-12	2
2126	2123.48	2.52	13-12-13-12-13	1
2122	2122.30	-0.30	12-13-12-13-12	1
2120	2120.12	-0.12	13-13-12-13-12	2
2117.5	2117.86	-0.36	13-13-12-13-13	1
2111	2109.46	1.54	12-13-13-12-12	2
2109	2107.50	1.50	13-13-13-12-12	2
2106.5	2105.65	0.85	13-12-13-13-12	2
2104.5	2103.55	0.95	13-13-13-12-13	2
2086	2085.23	0.77	12-13-13-13-12	1
2083	2082.52	0.48	13-13-13-13-12	2
2079.5	2079.67	-0.17	13-13-13-13-13	1

[a]Force constants obtained: f_R = 11.109 mdyn/Å, f_{Rr} = 1.499 mdyn/Å, f_r = 10.253 mdyn/Å and $f_{RR} = f_{rr} = 0$.

the 2164 cm^{-1} band was attributed to linear C_5. Shen and Graham[161] have recently assigned the 1544 cm^{-1} band to linear cumulenic C_4. They generated the C_4 by the photolysis of C_4H_2, diacetylene, C_4H_6, 1,3-butadiene C_4D_2, and various ^{13}C-substituted and deuterated isotopomers of C_4H_6.

The assignment of the 2164 cm^{-1} band to linear C_5 by this work,[162] enabled the detection of C_5 in the circumstellar shell[163] of the carbon star IRC+10216. Moazzen-Ahmadi, McKellar and Amano[164] have observed the rovibrational spectrum of gas-phase C_5 produced by a hollow cathode discharge in C_2H_2 + He and C_2H_4 + He mixtures by tunable diode laser spectroscopy. They obtained a gas-phase value of 2169.4 cm^{-1} for the band origin, a value of 5.4 cm^{-1} higher than the matrix-isolated value. Similar results were obtained by Heath et al.[165] on supersonically cooled carbon clusters produced by the laser vaporization of graphite.

It is worth noting that C_5 preserves its linear structure in the argon matrix. The argon lattice does not seem to distort the molecule to any detectable extent. Solid argon is known to have a face-centered cubic structure. If the Van der Waal radius of argon is assumed to be 1.91 Å,[166] then the removal of two adjacent argon atoms from the lattice would result in a cavity whose longest dimension would be 7.64 Å. If the covalent radius of a doubly bonded carbon atom is taken to be 0.67 Å,[166] then the length of the

C_5 molecule will be 6.7 Å and would allow it to fit in this cavity.

The relative intensities of the isotopomer bands as seen in Figure 3.2 appear to be anomalous since on statistical grounds one expects the variation of band intensities to be as given in column 5 of Table 1. Although the spectrum is symmetric about its midpoint, 2124 cm^{-1}, as expected, the intensities of, e.g., pure $^{12}C_5$ and $^{13}C_5$ molecules are clearly exaggerated. This is attributable to the fact that vaporization does not take place from an isotopic mixture at the atomic level but from a mixture of grains of essentially pure ^{12}C and ^{13}C graphite.

Conclusion

The 2164 cm^{-1} IR band has been conclusively shown to belong to the linear C_5 species. The assignment of the 1544 cm^{-1} band is less certain however. The utility of infrared spectroscopy and mixed-isotope studies in establishing the structure of small clusters has also been demonstrated.

CHAPTER IV

THE C_6 AND C_8 CLUSTERS

Introduction

Clusters such as C_6 and C_8 are present in very small quantities in graphite vapour when compared to species like C_2 and C_3. C_6 and C_8 were first detected by Drowart et al.[8] in graphite vapour by mass spectroscopy.

The earliest theoretical calculations on C_n molecules were carried out by Pitzer and Clementi.[67] They concluded that these molecules are linear and suggested that at about n = 10, cyclic structures might become more stable. They also predicted that linear molecules with odd n would have $^1\Sigma$ ground states and would be more stable than those with n even which have $^3\Sigma$ ground states. Similar conclusions were reached by Ewing and Pfeiffer[81-83] from single-determinant Hartree-Fock calculations on linear C_n molecules. A MINDO/2 study conducted by Slanina and Zahradnik[156] on C_n (n = 4-7) clusters with different geometries predicted that the most the most stable structure is non-linear. For C_6, for example, they considered the linear ($D_{\infty h}$), cyclic planar

(D_{6h}), square bipyramid (C_{2v}) and trigonal bipyramidal (D_{3h}) structures and found the square bipyramidal structure to be the most stable. An MNDO study by Bernholc and Phillips[81] considered neutral, positive and negatively charged chains and rings in the C_1 - C_{26} range. They concluded that the chain-like structure was most stable through C_9 while the monocyclic ring was the most stable structure in the C_{10} - C_{25} range for neutrals. The maximum stabilities were found to be at 10, 14, 18 and 23 atoms for neutrals.

Recent ab-initio calculations on C_6 by Raghavachari, Whiteside and Pople[80] concluded that the cyclic singlet structure with six π electrons (planar D_{3h}, ^1A) was the most stable structure with the linear $^3\Sigma_g^-$ structure lying about 10 kcal/mole higher. The vibrational frequencies calculated for the IR active σ_u stretches of the linear molecule were 2184 cm^{-1} and 1289 cm^{-1}. Other calculations by Ewing and Pfeiffer[83] at the Hartree-Fock level concluded that the linear C_6 structure was most stable. Recent calculations by Parasuk and Almlof,[87] using multiconfiguration self-consistent field (MCSCF) and multireference configuration interaction (MRCI) methods with large basis sets, predicted that the ground state structure of C_6 is linear with a cumulene-like electronic structure having $^3\Sigma_g^-$ symmetry. Similar results were obtained by Ott and Ray.[85] They too concluded that cyclic rings are preferred over linear chains for n>9.

Thompson et al.[86] have reported IR spectra of carbon vapour trapped in an argon matrix. Studies on highly enriched 95% ^{13}C together with annealing studies led them to assign the 1997 cm^{-1} and 1197 cm^{-1} bands to $^{12}C_6$ and the 1920 band to $^{13}C_6$. However, Kratschmer and Nachtigall[167], in a similar study did not observe a correlation between the 1997 cm^{-1} and 1197 cm^{-1} bands with annealing. They also recorded UV/VIS absorption spectra[88] and observed a series of bands in the 247-600 nm region which they assigned to C_4-C_9 clusters on the basis of growth and decay during annealing. The 394 nm and 529 nm bands were assigned to C_6 and C_8 respectively. A recent ESR study of graphite vapour in argon and neon matrices by Van Zee et al.[89] concluded that linear C_6, C_8 and C_{10} molecules were present in the matrices in their lowest $^3\Sigma$ states which are presumably their ground states. They also found evidence for two forms of C_{10}, possibly two slightly bent isomers.

Results

The infrared spectrum of the products of laser vaporized graphite was shown in the previous chapter in Figure 3.2. Figure 4.1 shows the difference spectrum (annealed minus unannealed) over the 2200-1800 cm^{-1} region after strong annealing. The negative peaks decrease in intensity upon annealing while the positive ones increase.

Upon annealing the matrix, it was observed that the 2164 cm^{-1} and 2039 cm^{-1} bands decreased in intensity, while the 1998 cm^{-1} band increased sharply. The 1952 cm^{-1} band grows slightly with annealing and then decreases.

The isotopic substitution method outlined in the previous chapter is then used to assign these bands. As mentioned earlier, for linear clusters, the various isotopomer bands are expected to lie in an ~80 cm^{-1} interval lower in energy from the ^{12}C cluster band. The number of isotopomers expected for linear C_n carbon clusters in the n=3 to 8 range are 6 for C_3, 10 for C_4, 20 for C_5, 36 for C_6, 72 for C_7 and 136 for C_8. This implies that as the cluster size increases, the isotopomer bands must become increasingly crowded in the ~80 cm^{-1} interval specified by the Teller-Redlich criterion. Table 3 gives the expected average densities for linear clusters from C_3 to C_8. For linear C_6, a band is predicted about every 2 cm^{-1}, whereas for linear C_8 a band is expected about every 0.5 cm^{-1}.

Figure 4.2 gives the unannealed spectra for ^{12}C products and ^{12}C:^{13}C mixed products in the 2070-1930 cm^{-1} range. The three major ^{12}C product peaks appear at 2039 cm^{-1}, 1998 cm^{-1} and 1952 cm^{-1}. In the mixed isotope spectrum the six isotopomer bands built on the 2039 cm^{-1} band are readily seen. Strikingly, in the mixed isotope spectrum the 1998 cm^{-1} and 1952 cm^{-1} ^{12}C parent peaks and their isotopomer partners appear to have disappeared. In fact they

Figure 4.1

Difference spectrum [annealed (35 K) - unannealed] of ^{12}C laser-ablation products in an argon matrix.

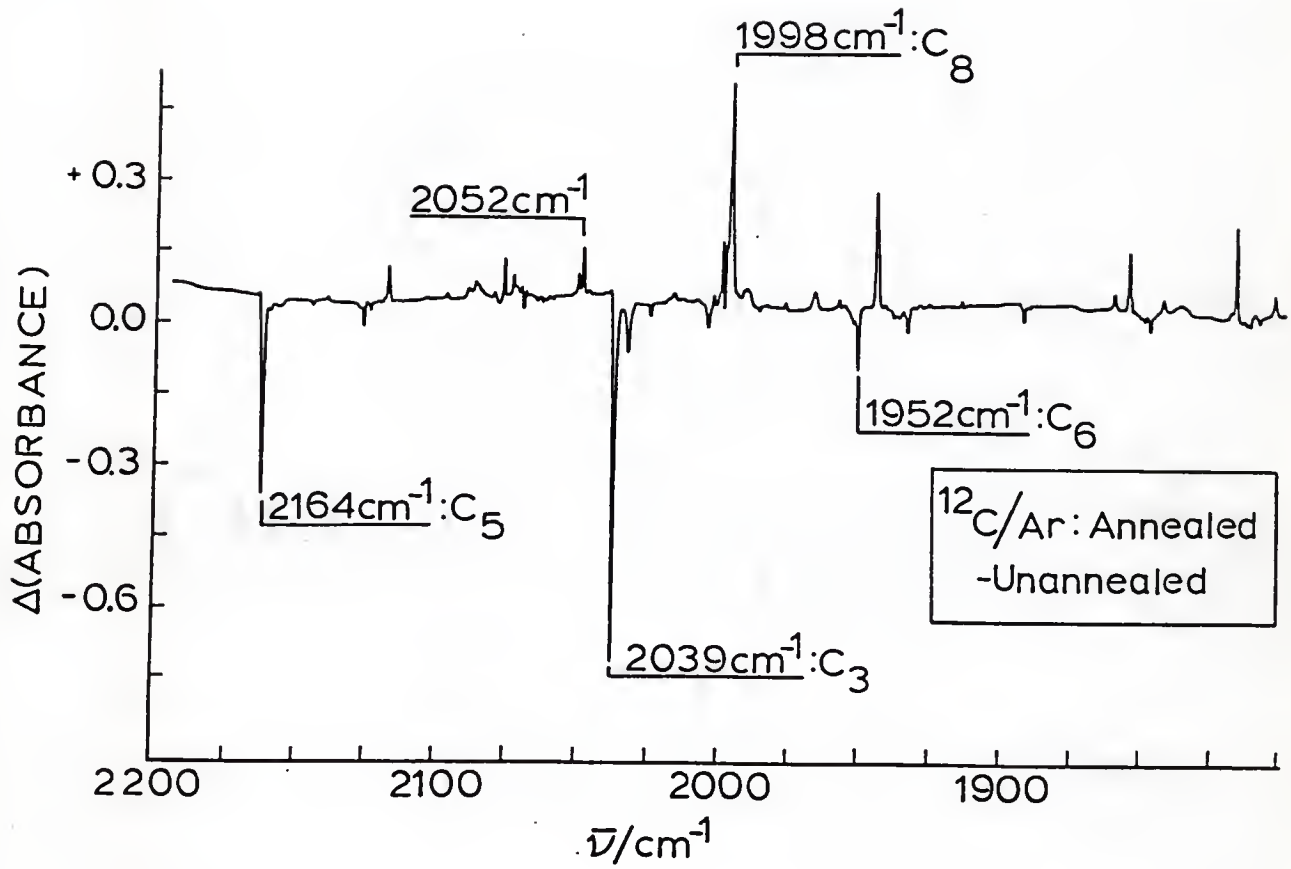
1998cm⁻¹:C8
2052cm⁻¹
+0.3
0.0
-0.3
-0.6
Δ(ABSORBANCE)
1952cm⁻¹:C6
2164cm⁻¹:C5
12C/Ar: Annealed
-Unannealed
2039cm⁻¹:C3
2200
2100
2000
1900
ν̄/cm⁻¹

TABLE 3

Expected Number of Isotopomers for Linear Carbon Clusters.

Cluster	Number of Bands	Band Density (Bands/cm^{-1})
C_3	6	0.075
C_4	10	0.125
C_5	20	0.25
C_6	36	0.45
C_7	72	0.90
C_8	136	1.725

Figure 4.2

Infrared spectra over the 2070-1930 cm^{-1} range of ^{12}C products (lower spectrum) and ^{12}C:^{13}C isotopically mixed products (upper spectrum) isolated in unannealed argon matrices at 12 K showing the six C_3 isotopomeric bands. Resolution = 0.25 cm^{-1}.

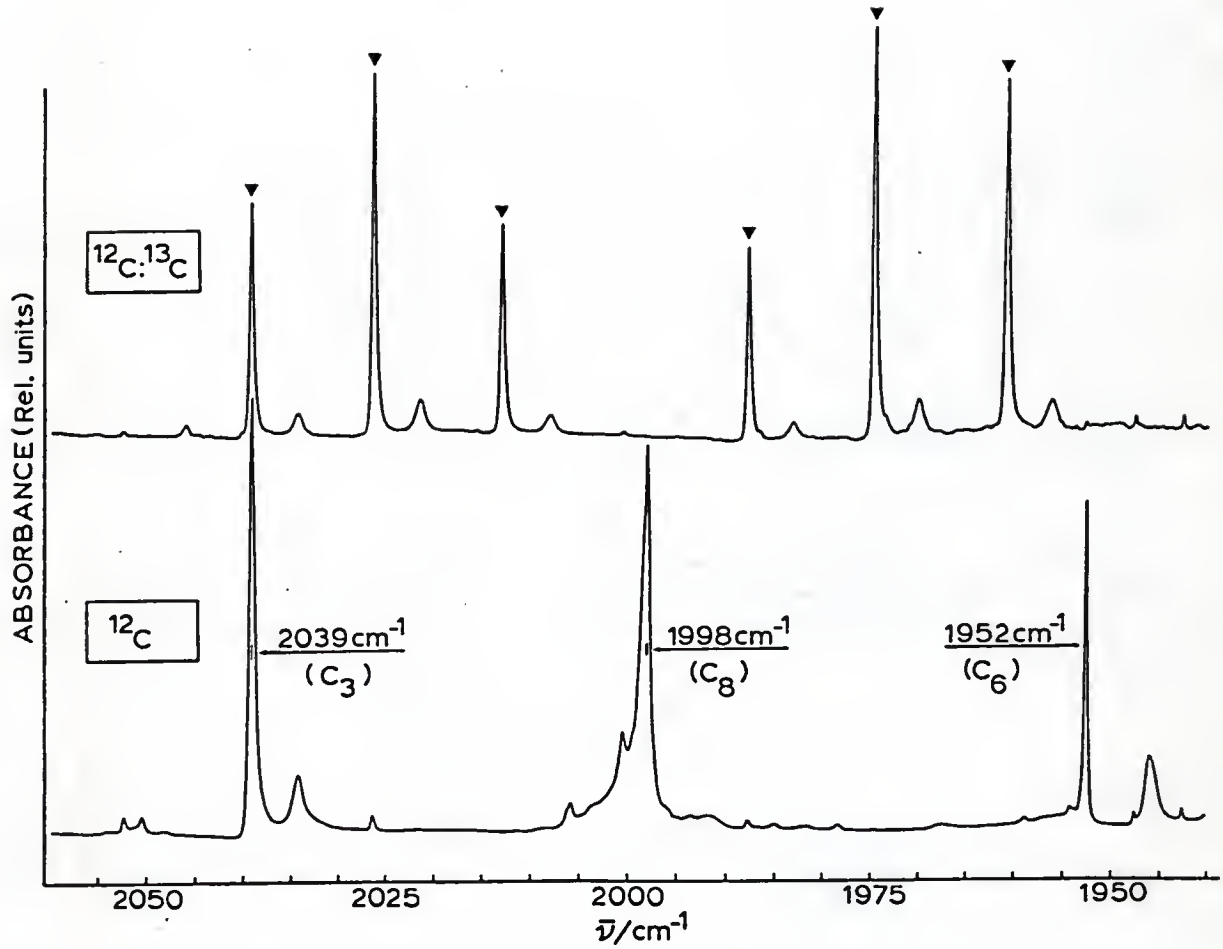
^{12}C:^{13}C
^{12}C
2039cm^{-1}
(C_3)
1998cm^{-1}
(C_8)
1952cm^{-1}
(C_6)
ABSORBANCE (Rel. units)
2050
2025
2000
1975
1950
$\bar{\nu}$/cm^{-1}

have just diminished greatly in intensity. The 1952 cm^{-1} is just barely visible in the mixed isotope run, but becomes easily discernable upon absorbance scale expansion (cf. Fig. 4.3). Its isotopomer partners stretch down to 1877 cm^{-1}, 75 cm^{-1} away. However, the isotopomeric peaks based on the 1998 cm^{-1} band are lost in the baseline in an unannealed matrix. With strong annealing, they emerge from the baseline and are readily recognized (cf. Fig. 4.4). Thompson et al.[86] have shown that the ^{13}C partner to the species responsible for the 1998 cm^{-1} band absorbs at 1920 cm^{-1}, a spread of 78 cm^{-1}. By tracking the behaviour of the bands in the overlap region (1952-1920 cm^{-1}) with progressive annealing, it was possible to decide which bands belong to the 1998 cm^{-1} set and which to the 1952 cm^{-1} set. The 1952 cm^{-1} set could be readily identified in the unannealed spectrum and their intensities changed little upon annealing. In contrast, the 1988 cm^{-1} set was barely discernable in comparison to the 1952 cm^{-1} set in the unannealed matrix, and grew substantially in the annealing process until their intensities were comparable to the 1952 cm^{-1} set. The two band systems overlap in the 1952-1920 cm^{-1} region as seen in Figure 4.4. Thus the annealing study allowed one to distinguish between the two sets of bands. The band density for the 1998 cm^{-1} set is markedly higher (~1.4 bands/cm^{-1}) than for the 1952 cm^{-1} set (~0.47 bands/cm^{-1}). It can be seen in Table 3, that from the band density criterion alone,

Figure 4.3

Infrared spectra over the 1980-1870 cm^{-1} range of ^{12}C products (lower spectrum) and ^{12}C:^{13}C isotopically-mixed products (upper spectrum) isolated in unannealed argon matrices at 12 K showing the more prominent C_6 isotopomer bands (cf Table 5). Resolution = 0.25 cm^{-1}.

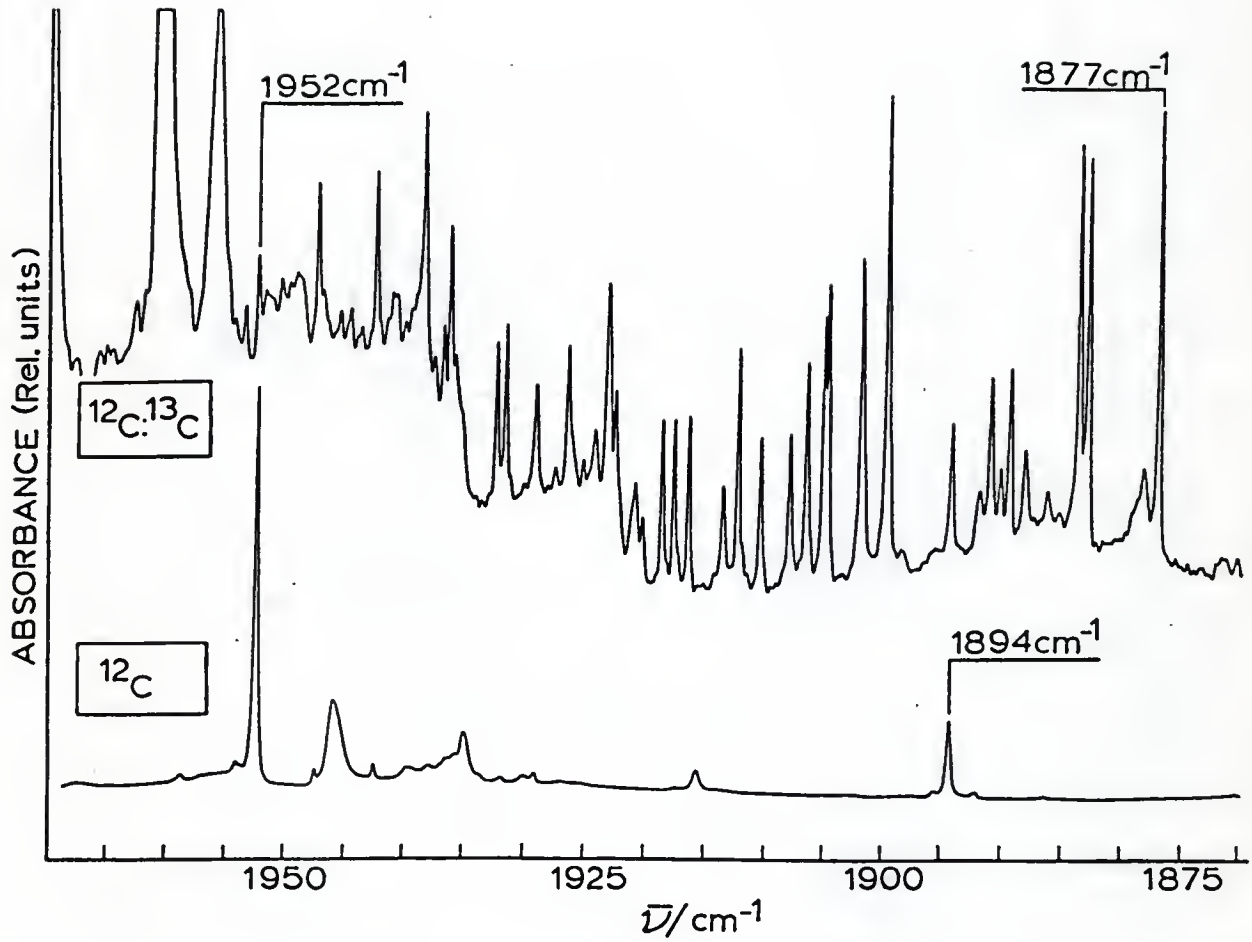
1952cm-1
1877cm-1
12C:13C
12C
1894cm-1
ABSORBANCE (Rel. units)
1950
1925
1900
1875
ν̄/ cm-1

Figure 4.4

Infrared spectra over the 2000- 1920 cm^{-1} range of ^{12}C products (lower) in an unannealed argon matrix. Upper spectrum shows the IR of the ^{12}C:^{13}C mixed products in argon at 12 K after annealing to 35 K for 15 min. Resolution = 0.25 cm^{-1}. Note the increased density of bands compared to Figs. 4.2 and 4.3.

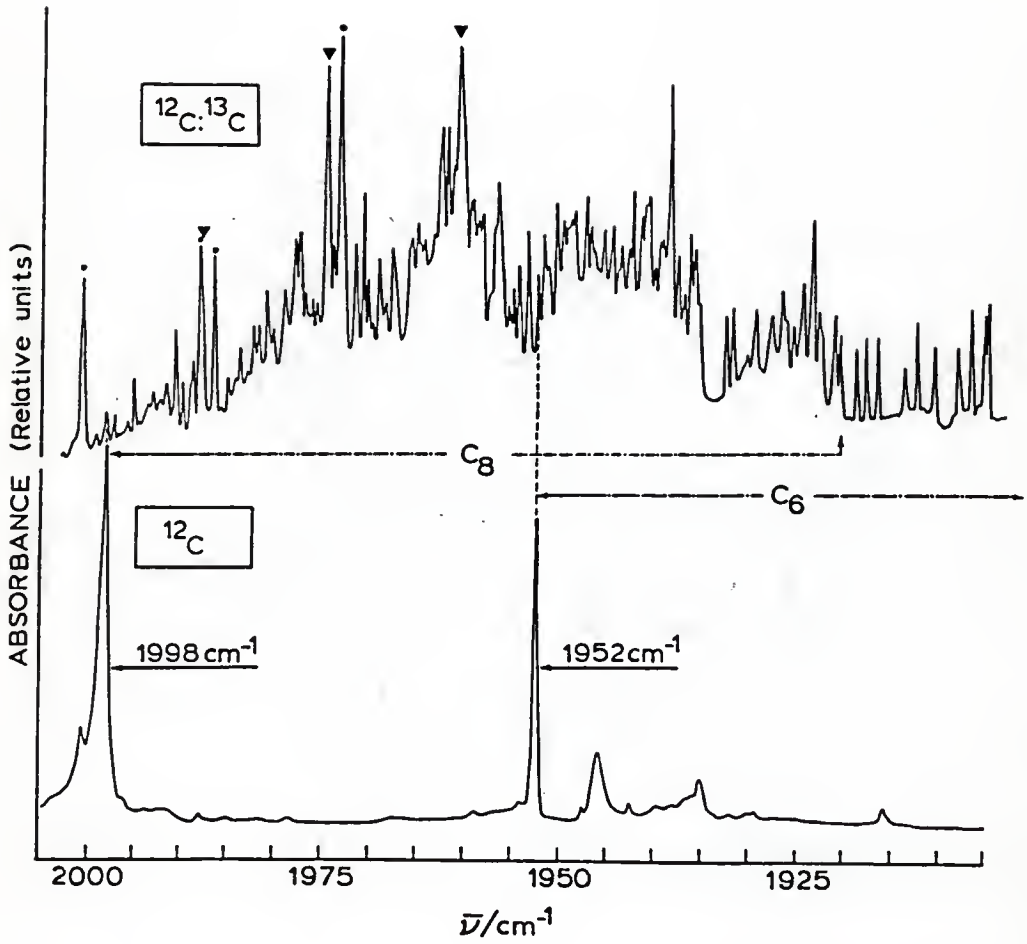
$^{12}C:^{13}C$
C_8
C_6
^{12}C
1998 cm^{-1}
1952 cm^{-1}
ABSORBANCE (Relative units)
2000
1975
1950
1925
$\bar{\nu}$/cm^{-1}

the 1998 cm^{-1} band cannot be ascribed to a linear cluster smaller than C_8. The observation of 35 bands in the 1952 cm^{-1} set (linear C_6 has 36 isotopomers) spread over a 75 cm^{-1} (1952-1877 cm^{-1}) interval strongly suggests that this band could be due to linear C_6.

This attribution nicely explains the apparent disappearance of the 1998 cm^{-1} band and the great diminution of the 1952 cm^{-1} band upon isotopic substitution. For linear C_8 the intensity originally concentrated in the $^{12}C_8$ band must be spread among 136 isotopomer peaks, while for linear C_6 it must be spread among only 36 isotopomer peaks. So, even though the ^{12}C run shows similar intensities for the 2039 cm^{-1}, 1998 cm^{-1} and 1952 cm^{-1} peaks, complete isotopic substitution would reduce the individual isotopomeric peak intensities to ~1/6 (C_3), 1/136 (C_8) and 1/36 (C_6) the intensity of the respective ^{12}C parent.

It is possible to use the isotopic intensity diminution in a semi-quantitative way to determine the number of carbons (n) in a linear cluster.[1] The following relation with C_3 is used as the internal standard:

$$I(^{12}C_3)/I(^{12}C_n) = (N_3/N_n)\ \ (I^i(C_3)/I^i(C_n)) \qquad (1)$$

where $I(^{12}C_3)$ and $I(^{12}C_n)$ are the intensities of the ^{12}C

[1] This approach was conceived by a colleague, Dr. Jan Szczepanski.

parents for the major IR bands due to C_3 (i.e., 2039 cm^{-1}) and the unknown C_n; N_3 and N_n are the number of possible isotopomers for C_3 and C_n, respectively; and $I^i(C_3)$ and $I^i(C_n)$ are the intensities of the ^{12}C parent peaks in the mixed isotope spectrum. Expressions giving the possible number of isotopomers for an even numbered linear cluster containing n atoms are[168]

$$N_n = 2(2N_{n-2} - 2^{n/2-2}) \qquad (2)$$

and $N_{n'} = 2N_n$ where n' is odd and equal to n + 1. Obviously, $N_1 = 2$ and $N_2 = 3$. Thus $N_3 = 6$ possible isotopomers. By solving (1) for N_n and substituting it into (2), it is possible to determine n. To test this approach the data for C_5 (cf. Fig. 4.4) were used: $I(^{12}C_5)/I(^{12}C_3) = 0.49$, $I^i(C_3)/I^i(C_5) = 6.2$ from which $N_n = 18.2 \approx 20$. From (2) this gives n = 5. For the 1952 cm^{-1} band intensity data we find $I(^{12}C_5)/I(^{12}C_3) = 0.51$, $I^i(C_3)/I^i(C_n) = 11.3$, so that $N_n = 34.6 \approx 36$. Thus n = 6. This is in agreement with the conclusion drawn above from the band density data.

Normal Coordinate Analysis

Thirty-five isotopomeric peaks lying between 1952 cm^{-1} and 1877 cm^{-1} are observed (36 are expected for chainlike

C_6) and are listed in Table 4. The normal coordinate analysis was done by fitting five force constants to sixteen of the bands (marked with asterisks in Table 4), 10 from the ^{12}C end and 6 from the ^{13}C end of the isotopomer list. The force constants varied to effect the fit were: f_R, outer bond stretching force constant, f_r, next inner bond stretch, f_m, middle bond stretch, f_{rm}, interaction between r and m bond stretches and f_{Rr}, interaction between R and r bond stretches. The program[160] used to obtain the fit allowed all five force constants to be varied independently until the best fit with the experimental data was obtained. The fit described here is for a slightly bent C_6 (hence the use of the term "chainlike" instead of linear). The best fit to a linear C_6 geometry was considerably worse, with a RMS deviation of 2.2 cm^{-1} and as shown in Table 5. In comparison, the best fit for the bent structure (Table 4) had a RMS deviation of 1.79 cm^{-1}.

A number of different bent structures were tried and the best fit obtained for the structure described below. Let us consider the C atoms of the molecule numbered in sequence: C_1-C_2-C_3-C_4-C_5-C_6. Keeping the C_1-C_2, C_3-C_4 and C_5-C_6 bonds parallel, the C_2-C_3 and C_4-C_5 bonds are bent 15 degrees away from linear in opposite directions (i.e. trans-like) and further twisted 7 degrees out-of-plane in an opposite sense. Although a number of bending angles were tried, the final choice of angles may not be unique, and it

TABLE 4

Observed and Calculated Isotopomer Stretching Frequencies for Chain-like C_6 in an Argon Matrix.[a]

Observed[b] ν/cm^{-1}	Calc'd ν/cm^{-1}	Diff. $\Delta\nu/cm^{-1}$	Observed ν/cm^{-1}	Calc'd ν/cm^{-1}	Diff. $\Delta\nu/cm^{-1}$
*1952.5	1950.4	2.1	1908.0	1907.3	0.7
*1947.5	1945.1	2.4	1906.5	1906.5	0
*1942.5	1941.5	1.0	1905.2	1905.6	-0.4
*1938.5	1942.4	-3.9	1904.7	1905.3	-0.6
*1937.0	1938.5	-1.5	1901.9	1901.8	0.1
*1936.4	1934.9	1.5		1901.6	0.3
*1932.4	1932.8	-0.4	1899.7	1900.5	-0.8
*1931.5	1934.3	-2.8	1894.3	1895.9	-1.6
*1929.2	1928.5	0.7	1892.0	1895.3	-3.3
*1926.5	1924.6	1.9	1891.0	1895.1	-4.1
1923.3	1923.3	0	1890.2	1892.4	-2.2
1922.5	1922.0	0.5	1889.5	1891.5	-2.0
1918.2	1915.7	2.5	*1888.2	1888.3	-0.1
1917.5	1915.2	2.3	*1886.3	1885.1	1.2
1916.5	1914.4	2.1	*1883.7	1882.7	1.0
1913.5	1913.2	0.3	*1883.0	1883.8	-0.8
1912.3	1912.1	0.2	*1878.3	1877.9	0.4
1910.3	1911.7	-1.4	*1877.2	1873.9	3.3

[a]Force constants found: f_R=10.9367 mdyn/Å; f_r=9.4468 mdyn/Å; f_m=9.7160 mdyn/Å; f_{Rr}=1.1401 mdyn/Å; f_{rm}=0.9306 mdyn/Å (R = outer bond, r=inner bond, m=middle bond).

[b]Bands marked * were used in the initial fitting to determine force constant parameters.

TABLE 5

Observed and Calculated Isotopomer Stretching Frequencies for Linear C_6 in an Argon Matrix.[a]

Observed[b] ν/cm^{-1}	Calc'd ν/cm^{-1}	Diff. $\Delta\nu/cm^{-1}$	Observed ν/cm^{-1}	Calc'd ν/cm^{-1}	Diff. $\Delta\nu/cm^{-1}$
*1952.5	1951.4	1.1	1908.0	1908.5	-0.5
*1947.5	1947.4	0.1	1906.5	1907.6	-1.1
*1942.5	1944.6	-2.1	1905.2	1905.6	-0.4
*1938.5	1942.2	-3.7	1904.7	1904.6	0.1
*1937.0	1939.6	-2.6	1901.9	1902.9	-1.0
*1936.4	1936.1	0.3		1902.9	-1.0
*1932.4	1934.6	-2.2	1899.7	1901.8	-2.1
*1931.5	1932.8	-1.3	1894.3	1897.8	-3.5
*1929.2	1928.4	0.8	1892.0	1896.3	-4.3
*1926.5	1925.3	1.2	1891.0	1895.9	-4.9
1923.3	1924.0	-0.7	1890.2	1894.9	-4.7
1922.5	1923.4	-0.9	1889.5	1892.4	-2.9
1918.2	1915.6	2.6	*1888.2	1889.7	-1.5
1917.5	1914.9	2.6	*1886.3	1886.4	-0.1
1916.5	1914.7	1.8	*1883.7	1884.8	-1.1
1913.5	1914.4	-0.9	*1883.0	1882.4	0.6
1912.3	1914.2	-1.9	*1878.3	1878.1	0.2
1910.3	1913.8	-3.5	*1877.2	1874.9	2.3

[a]Force constants found: f_R=11.3064 mdyn/Å; f_r=8.7636 mdyn/Å; f_m=9.0604 mdyn/Å; f_{Rr}=1.1636 mdyn/Å; f_{rm}=0.6225 mdyn/Å (R = outer bond, r=inner bond, m=middle bond).

[b]Bands marked * were used in the initial fitting to determine force constant parameters.

is possible that other choices might give a comparable fit. This distortion from linear geometry is possibly the result of packing stresses induced by the argon matrix. The bond lengths of the C-C bonds used in this calculation were obtained from Raghavachari's[80] estimation of the bond lengths of a cumulenic structure. The outer bonds C_1-C_2 and C_5-C_6 were assumed to be 1.3 Angstroms while the remaining three inner bonds were assumed to be 1.266 Angstroms. It is interesting to note in this regard that C_5, which is known to be linear fits easily into a vacancy created by the removal of two adjacent argon atoms, but linear C_6 will not fit into this cavity.

No normal coordinate analysis was attempted for C_8 since the large number of very closely spaced bands precludes any meaningful fit.

Discussion

The assignments of the 1952 cm^{-1} and 1998 cm^{-1} bands to C_6 and C_8, respectively, differ from the the assignments proposed by Thompson et al.[86] Using intensity changes upon thermal annealing and partial isotopic substitution (5% ^{12}C and 95% ^{13}C) these authors had attributed the 1998 cm^{-1} band to C_6 and the 1952 cm^{-1} band to C_5. Because the 1998 cm^{-1} band increases with annealing while the 2039 cm^{-1} (C_3) band decreases, these authors suggested that two C_3 clusters

react in the matrix to form C_6. Given the assignments of this work, it seems likely that C_3 reacts with C_5 (both of whose bands decrease upon annealing) to form C_8. Whether two C_3's react to form C_6 is more problematic, since the 1952 cm^{-1} (C_6) band increases slightly upon annealing and then decreases upon stronger annealing. Perhaps two C_3's react to form C_6, which if the matrix becomes soft enough at higher annealing temperatures, can react further to form larger clusters (C_7, C_8, C_9, etc.). This possibility needs to be pursued further. At any rate, it is clearly evident from the change in the C_6 peak intensity upon annealing that the majority of the C_6 observed is formed in the gas phase and not in the matrix as a consequence of some chemical reaction.

The assignment proposed here for C_6 is in good accord with recent theoretical predictions. Raghavachari et al.[80] calculated IR-active frequencies of 2184 cm^{-1} and 1289 cm^{-1} for cumulene-like linear C_6 and 1173 cm^{-1} and 1056 cm^{-1} for acetylene-like linear C_6. The experimental frequencies of 1952 cm^{-1} and 1197 cm^{-1} are within 12% and 8%, respectively of the predicted cumulenic C_6 values. They are sufficiently distant from the acetylenic-C_6 values to conclude that the cumulenic form is the structure favoured by linear C_6. This conclusion is further supported by the theoretical stability calculations. They show that the cumulenic form is 33.3 kcal./mole more stable than the acetylenic structure.[80] It

is worth recalling that some theoretical calculations predict cyclic C_6 structures considerably more stable than the linear forms: the D_{3h} distorted ring lies lowest with the symmetric D_{6h} ring 3.5 kcal/mole higher. The cumulenic linear structure lies at 19.3 kcal/mole. The natural question then is: why do we observe linear C_6 rather than cyclic C_6?

The answer has been provided by Van Zee et al.,[89] who estimate that for equilibrium concentrations in a laser vaporization plume at 3000 or 4000 K with a ΔH = +10 kcal/mole (for the conversion of the D_{3h} ring to the cumulinic linear form) the K_p ratio (= P_{linear}/P_{ring}) will be 50 at 3000 K and 200 at 4000 K. Thus the concentration of the linear form in the vapour before deposition is expected to be far greater than that of the cyclic form, and our observation of the linear form is understandable. It will be of interest to determine whether the more stable cyclic structure may be formed from the linear upon vigorous matrix annealing.

No comparison of the experimental C_8 frequency with recent theoretical values is possible as none has been reported for linear C_8. However, comparison to a simple model is instructive. Halford[169] has given an expression for the stretching frequencies of a model linear chain which has force constants (k) for all bonds. For N number of atoms of mass m in the chain, the n stretching frequencies are given

by

$$\nu_n = (k/\pi^2 m)^{1/2} \sin(n\pi/2N) \qquad (3)$$

where n = 1, 2,...,N-1 and only the even n frequencies will be IR active. Choosing the C_3 frequency (2039 cm^{-1}) to calibrate this expression yields $(k/\pi^2 m)^{1/2}$ = 2354.5 cm^{-1}. Then the expression gives for C_5: 2239 cm^{-1} (2164 cm^{-1}) and 1384 cm^{-1} (1544 cm^{-1}); experimental frequencies are given in parentheses. For C_6: 2039 cm^{-1} (1952 cm^{-1}) and 1177 cm^{-1} (1197 cm^{-1}); for C_8: 2175 cm^{-1} (1998 cm^{-1}), 1665 cm^{-1} and 902 cm^{-1}. Thus even this simple expression mimics the placement of the highest energy IR band of C_8 between the C_5 and C_6 bands, as we find. Although further work is needed for a firm conclusion, it appears that C_8 is also present in the cumulenic form.

Conclusion

In summary, evidence from infrared spectroscopic studies has led to the assignment of the 1952 cm^{-1} and 1998 cm^{-1} bands to the C_6 and C_8 clusters, respectively. The structures of these species were found to be probably linear or possibly slightly bent with cumulenic-type bonding. The bending of the molecule could be due to a matrix effect. It is interesting to note that linear C_6 will not fit in a

vacancy left by the removal of two adjacent argon atoms as C_5 will. The limitations of the mixed isotopomer technique become evident for the larger C_8 cluster. As the size of a linear or chain-like cluster increases, its number of isotopomers increases very rapidly and since these bands are spread over ~80 cm^{-1}, they become too closely spaced to make any fit to calculated frequencies meaningful.

CHAPTER V

THE IONIC C_5^+ CLUSTER

Introduction

The laser vaporization of graphite is known to produce ions in addition to the dominant neutral species. The earliest work was reported by Honig[6] in 1954 and by Dornenburg et al.[170] in 1961. Furstenau, Hillenkamp and Nitsche[9] have observed positive and negative ions from the laser vaporization of thin carbon foils. They found that the distribution of laser-induced carbon cluster ions indicated an upper limit for the electron temperature of the carbon plasma to be between 40,000 and 60,000 K, corresponding to 3-5 eV. For $C_n^{\pm}$ clusters with $n < 9$, they found that the odd-even rule with $\Delta n = 2$ is satisfied. In the mass spectrum, the positive ions were found to have maxima for odd n while the negative ions for even n. This was followed by work by Furstenau and Hillencamp[10] in which the above conclusions were confirmed.

Rohlfing et al.[11] reported the generation of a supersonic beam of ionic carbon clusters by laser

vaporization of graphite within the throat of a pulsed nozzle. They observed clusters C_n for n = 1-190 with a distinctly bimodal distribution: (i) Both even and odd clusters for C_n, $1 \leq n \leq 30$; and (ii) only even clusters C_{2n}, $20 \leq n \leq 90$. The alterations in the observed C_n^+ signals were interpreted on the basis of cluster formation and stability arguments. Linear carbon clusters generated by a spark source discharge were studied by Leleyter.[171] For C_n^+, odd n values were found to be more abundant, while for C_n^-, the even values were more abundant with negative ion intensities dropping rapidly for n>9.

Bloomfield et al.[136] have produced carbon cluster ions both by the photoionization of neutral clusters using 193 nm radiation and directly by the vaporization of graphite with a high power laser. For the former, a laser power of approximately 2×10^9 W/cm^2 was found to be adequate, while cluster ion production required two to three times this intensity. The laser-generated C_n^+ spectra were found to be similar to those obtained by Furstenau and Hillencamp.[10] However, the photoionized spectra were different for clusters with greater than thirty atoms. In the direct C_n^+ production, there was a progressive fall off in intensity with increasing cluster size with only a weak even-odd alternation in abundance. However, when neutral C_n clusters were ionized, only even clusters were seen to be formed. For the negative clusters, an even-odd alternation was observed

in the abundances of the clusters. For the lighter clusters, magic numbers were found to exist for n = 5, 10, 12, 16, 18 and 22. The negative ion data were not in agreement with that obtained by Furstenau and Hillencamp, who observed maxima only for even n with rapidly declining intensity beyond n=9.

Geusic et al.[137] have conducted detailed studies on the photofragmentation of carbon cluster cations containing between 3 and 20 atoms. They observed that for most C_n^+, the loss of C_3 was the dominant reaction channel, due to the special stability of C_3.[78,172,173] C_3 loss is not necessarily the dominant loss channel from all metastable C_n^+ ions.[174] For example, C_{11}^+ decomposes mainly via C_1 elimination, the C_3 loss being the minor pathway. The unique loss of one carbon atom from C_{11}^+ probably reflects the special stability of the C_{10}^+ ion which has been predicted to have a ring structure.[79] C_5^+ was found to fragment to C_2 and C_3^+, as C_3 has a lower ionization energy than C_2. The structure of small carbon cluster ions has been studied by reacting the ions with small hydrocarbons,[100] HCN,[99] D_2 and O_2.[98] It was found that the reactivity of the cluster ions undergoes an abrupt change as the cluster size increases from C_9 to C_{10}. This has been rationalized on the basis of the cluster changing its structure from a chain-like to a cyclic form.

On the theoretical front, Bernholc and Phillips[81] have carried out self-consistent modified neglect of differential overlap (MNDO) calculations on neutral, positive and negative chains and rings in the C_2-C_{26} range. The most stable positive ions were found to be C_{11}^+, C_{15}^+, C_{19}^+ and C_{23}^+; the most stable negative ions were C_{14}^-, C_{18}^- and C_{22}^-. The observed (4n+3) periodicity of C_n^+ clusters is in conformity with Huckel's rule.

Islam and Ray[175] have carried out a Hartree-Fock study on ionized linear, three-dimensional and ring-shaped clusters. For C_n^+ clusters, they observed that clusters with n = 7, 11, 15 and 19 were the most stable in agreement with the results of Rohlfing et al.[11] The stability of ionized clusters was examined by computing the fragmentation energy of the clusters.

The technique of matrix isolation spectroscopy has been applied sparingly to the study of ionic species until recently, partly because of the sensitivity problem, common to all ion spectroscopies, but probably more importantly due to the matrix perturbation problem for charged species. The interaction of charged species with most host matrices may be sufficiently strong so that either no spectrum is obtainable or the spectrum obtained tells little about the isolated molecular ion. For these reasons, the only matrices generally found suitable for studies of isolated ions are inert gas matrices.

Very little work has been done on carbon cluster ions in matrices. Milligan and Jacox[148] have prepared C_2^- by the VUV photolysis of acetylene in argon matrices. Froch[149] too has generated C_2^- in argon, krypton and Xe matrices by the X-irradiation of acetylene and studied its emission spectrum. Brus and Bondybey[176] have measured the laser excitation spectrum of C_2^- produced by the photolysis of acetylene in neon, argon, krypton and xenon matrices, and provided an explanation for the formation of the ion, using 121.6 nm radiation as the ionizing radiation. Forney, Althaus and Maier[139] have recently recorded the electronic absorption spectrum of C_2^+ in neon matrices produced by the the VUV photolysis of acetylene and halogenated acetylenes with the best results being obtained with chloroacetylene.

A considerable amount of work has been done on the spectroscopy of benzenoid cations in matrices. Work on the IR spectroscopy of ions in matrices was recently reviewed by two of its leading practitioners, Andrews[177] and Jacox.[178] The electronic spectroscopy of ions, both in the gas phase and in matrices, has been reviewed by Miller and Bondybey[179] and Bondybey and Brus.[180]

Experimental

The experimental procedure used in studying the C_5^+ ion was very similar to that described earlier. A modification

was required to differentiate between ions and neutrals. It is well known[9,10] that positive and negative ions are produced in the laser vaporization process.

Two approaches were used to determine whether the 2052 cm^{-1} band was due to a neutral or an ionic species. In the first, a small copper wire ring (~2 cm dia.) was mounted ~0.5 cm in front of the CsI sample window and electrically insulated from it and its copper mount. Small positive and negative voltages (upto ±48V.) were applied to the ring to attract (or repel) carbon cluster ions formed in the laser vaporization process. In the second approach, a small tungsten filament acting as an electron gun, mounted in close proximity to the sample window, was used to neutralize any positive cluster ions present. Simultaneously, a band at 904 cm^{-1}, ascribed to the ArH^+ species,[155] was also monitored.

Results

Laser vaporization of graphite followed by trapping of the vaporized products in an argon matrix results in the appearance of many infrared bands. In the 1970-2060 cm^{-1} region (cf. Fig 5.1, bottom spectrum) two prominent bands at 2039 cm^{-1} and 1998 cm^{-1} together with a number of less intense bands, including one at 2052 cm^{-1} can be readily observed in an unannealed matrix. The 2039 cm^{-1} is known[86]

to belong to C_3 and the 1998 cm^{-1} band was assigned to chain-like C_8 in the previous chapter. Upon annealing, the 2052 cm^{-1} band increases in intensity.

The evidence for the assignment of this band to an ionic species is the following. In Figure 5.2 are shown the spectra observed in two separate runs using a positive or negative voltage on the ring during deposition. Figure 5.2 shows the result obtained with +48 V and -48 V on the ring. The laser focus and other conditions were similar although the overall absorbance of the two varied substantially due to different deposition times. To compensate for this, the ratio of the 2052 cm^{-1} band intensity to the 2039 cm^{-1} (neutral C_3) band intensity was determined. For the -48 V. ring potential the ratio was 0.63, while for the +48 V. it was 0.17. The ratio is expected to be larger for the negative potential if the species producing the 2052 cm^{-1} band is a positive ion, as we observe. As confirmation of this, electron flow from the tungsten-filament electron gun caused the complete disappearance of this band, as well as the ArH^+ band[155] at 904 cm^{-1}.

For a 1:1 (^{12}C:^{13}C) mixed isotope sample, the top spectrum in Figure 5.1 was observed after annealing the matrix. The five bands marked with an inverted triangle are the isotopomers of C_3 (the sixth one lies at ~1960 cm^{-1}). The myriad of bands to lower energy of the 1998 cm^{-1} band are due[168] to a number of the 136 isotopomers belonging to

Figure 5.1

Bottom spectrum: Infrared spectrum of ^{12}C products in an unannealed argon matrix at 12 K showing prominent 1998 cm^{-1} C_8 band and 2039 cm^{-1} peak. Top spectrum: Infrared spectrum of products from a laser-vaporized 1:1 ^{12}C:^{13}C isotopic mixture in an annealed argon matrix 12 K showing C_3 isotopomer peaks ( ) and cyclic C_5^+ isotopomeric peaks ( ). Resolution = 0.25 cm^{-1}.

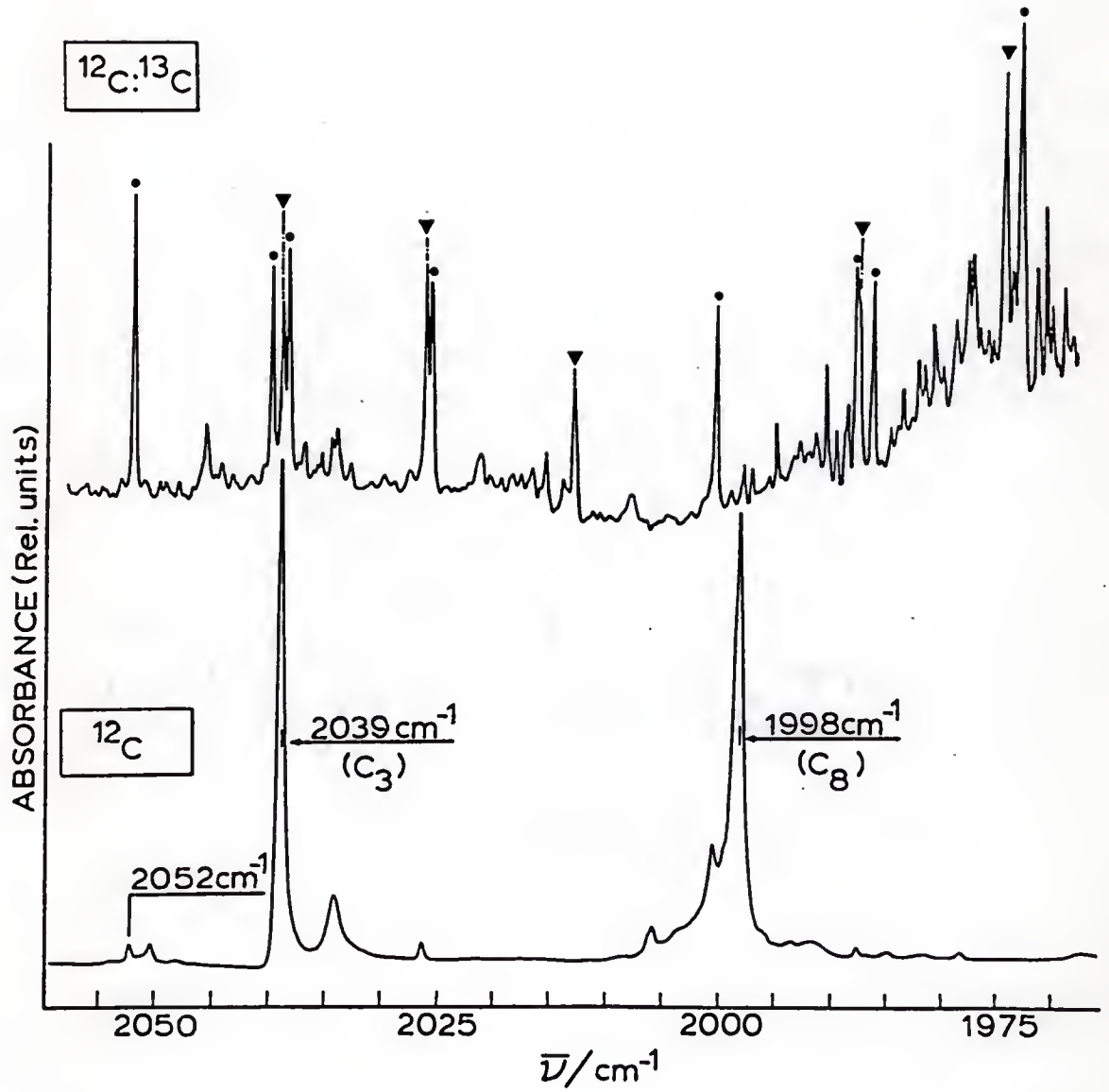
^{12}C:^{13}C
^{12}C
2039 cm^{-1}
(C_3)
1998cm^{-1}
(C_8)
2052cm^{-1}
ABSORBANCE (Rel. units)
2050
2025
2000
1975
$\bar{\nu}$/cm^{-1}

Figure 5.2

Left panel: Portion of infrared spectrum with +48.0 V. on the ring electrode during deposition showing the $^{12}C_5^+$ peak at 2052 cm^{-1} and neutral $^{12}C_3$ peak at 2039 cm^{-1}. Resolution = 1 cm^{-1}. Right panel: Portion of infrared spectrum with -48 V. on the ring electrode of an unannealed matrix of ^{12}C in argon at 12 K.

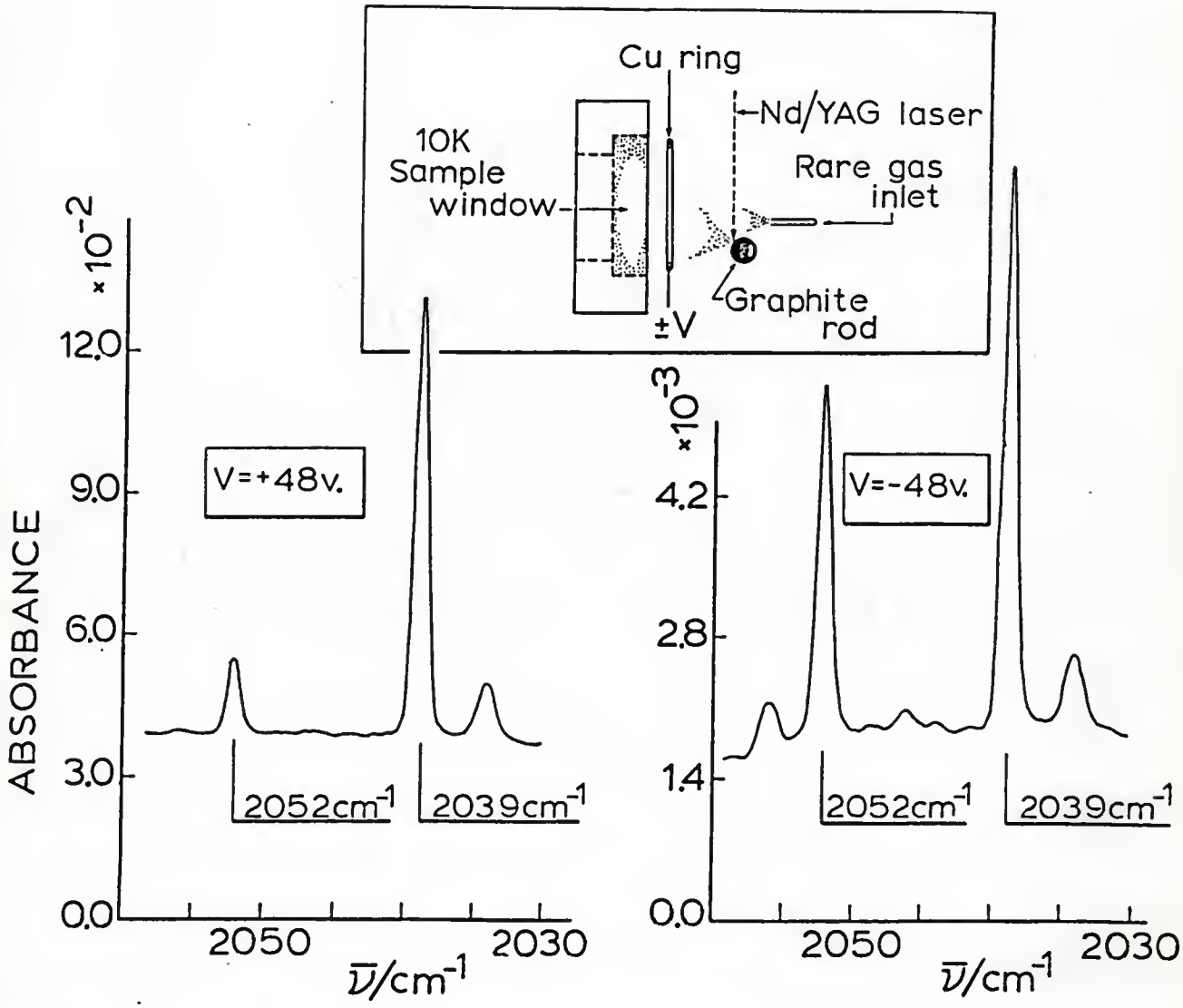
Cu ring
Nd/YAG laser
10K
Sample
window
Rare gas
inlet
±V
Graphite
rod
ABSORBANCE
×10⁻²
12.0
9.0
6.0
3.0
0.0
V=+48v.
2052cm⁻¹
2039cm⁻¹
2050
2030
ν̄/cm⁻¹
×10⁻³
4.2
2.8
1.4
0.0
V=-48v.
2052cm⁻¹
2039cm⁻¹
2050
2030
ν̄/cm⁻¹

linear C_8. Upon further annealing, these bands gain in intensity.

Apart from the known isotopomer bands due to C_3 and C_8, eight strong bands (marked with black dots) appear between 2052 cm^{-1} and 1973 cm^{-1}, a span of 79 cm^{-1}. It is perhaps worth noting the narrow width (FWHM = 0.5 cm^{-1}) of these bands. A series of runs was intially carried out at 1 cm^{-1} resolution, normally sufficient to resolve bands due to matrix isolated species. But with this resolution the group of three bands at ~2039 cm^{-1} appeared as a single band, as did the group of two bands at ~2026 cm^{-1}. This produced the apparent result that the two highest energy C_3 isotopomer peaks (2039 cm^{-1} and 2026 cm^{-1}) gained in intensity upon annealing while the band at 2013 cm^{-1} decreased. This perplexing result was only understood when the higher (0.25 cm^{-1}) resolution was used and the isotopomeric bands built on the 2052 cm^{-1} parent were resolved and distinguished from the bands due to the other species.

Table 6 lists the expected number of isotopomers for clusters from C_3 to C_8 having linear and cyclic structures. It can be seen that the cyclic C_5 structure possesses eight isotopomers. Only one infrared-active mode is expected for this species. A planar five-atom molecule belonging to the D_{5h} point group possesses five vibrational modes (four of which are doubly degenerate). Their symmetries and activities are a_1' (Raman-active), e_1' (IR-active), $2e_2'$

TABLE 6

Expected Number of Isotopomers for Linear and Cyclic Carbon Clusters.

Cyclic Cluster			Linear Cluster	
Cluster	Cyclic Symm.	Number of Bands	Cluster	Number of Bands
C_3	D_{3h}	4	C_3	6
C_4	D_{2h}	9	C_4	10
	D_{4h}	6		
C_5	D_{5h}	8	C_5	20
C_6	D_{3h}	20	C_6	36
	D_{6h}	13		
C_7	D_{7h}	22	C_7	72
C_8	C_{4h}	45	C_8	136

(Raman active) and e_2" (forbidden). The sole IR-active mode is a combination carbon-carbon stretching and bending mode.[154]

The presence of eight isotopomeric bands limits the possible geometries of the species giving rise to the 2052 cm^{-1} band to only three. They are 1) cyclic C_5 (D_{5h} symmetry), 2) trigonal planar C_4 (D_{3h} symmetry) and 3) pyramidal C_4 (C_{3v} symmetry). In order to determine which of these geometries is the carrier of the 2052 cm^{-1} band, a normal coordinate analysis on all three was performed and attempts made to fit the calculated bands to the observed ones. In the case of pyramidal C_4, calculations were carried out on ten structures with the angle between the C-C bond and the plane perpendicular to the principal three-fold rotation axis (θ) varied between 2 and 40 degrees. Unsatisfactory fits (rms deviations of all bands $\approx$ 3 cm^{-1} or greater) were obtained for all ten structures. Unsatisfactory fits were also obtained for the trigonal planar C_4 structure as well. Table 7 lists the results obtained for pyramidal and planar C_4 for θ = 25°. It can be seen that the fit is not good with a RMS deviation of 3.953 cm^{-1} from the experimental values. Table 8 lists the RMS deviations obtained for the various values of θ. The planar cyclic C_5 geometry, however, gave an excellent fit with reasonable force constants.

TABLE 7

Calculated Frequencies for Tetrahedral C_4 for $\theta = 25°$[a]

Calc. Freq. (ν/cm^{-1})	Obs. Freq. (ν/cm^{-1})	Difference ($\Delta\nu/cm^{-1}$)	Structure of Isotopomer	Stat. Wts.
2049.47	2052.25	-2.78	12-12-12-12	1
2046.54	2040.00	6.54	13-12-12-12	3
2039.89	2038.50	1.39	12-12-12-13	1
2022.77	2025.75	-2.98	13-12-12-13	3
1996.47	2000.50	-4.03	13-13-12-12	3
1993.45	1988.00	5.45	13-13-12-13	3
1986.85	1986.50	0.35	13-13-13-12	1
1969.06	1973.25	-4.19	13-13-13-13	1

[a] θ is the angle between the C-C bond and the plane perpendicular to the principal three-fold rotation axis.

TABLE 8

Calculated Fits for Pyramidal C_4.

Angle θ[a]	RMS Deviations
2	4.715
5	4.689
7	4.659
10	4.467
15	4.299
20	7.267
25	3.953
30	9.817
35	4.886
40	10.684

[a] θ is the angle between the C-C bond and the plane perpendicular to the principal three-fold rotation axis varied between two and forty degrees.

The calculated and observed frequencies are compared in Table 9. The rms deviation of all bands is 1.038 cm^{-1}; the worst fit band is 1.90 cm^{-1} off. The program[160] used to effect this fit permits the variation of all force constants specified until the best fit is obtained. In this case the six force constants specified were: f_R (bond stretch), f_θ (C-C-C angle bend), f_{RR}^A (adjacent bond stretch interaction), $f_{R\theta}^A$ (adjacent bond stretch-angle bend interaction), f_{RR}^{NA} (non-adjacent bond stretch interaction) and $f_{R\theta}^{NA}$ (non-adjacent bond stretch-angle bend interaction). A smaller number was tried but the fit obtained not nearly as good. The six force constants obtained are given in Table 8. The nonnegligible magnitude of the nonadjacent interaction force constants is not unexpected because of the combined stretch and bend components of the mode. The excellent fit obtained is strong evidence that the planar pentagonal C_5^+ cluster is responsible for the 2052 cm^{-1} IR band.

The relative intensities of the eight isotopomer peaks appear to be anomalous, since on statistical grounds one would expect the variation of band intensities to be as given in Table 8 (Col. 5). The intensities of pure $^{12}C_5^+$ and $^{13}C_5^+$ appear exaggerated since vaporization does not take place from an isotope mixture at an atomic level, but from a mixture of essentially pure ^{12}C and ^{13}C grains.

TABLE 9

Observed and Calculated Isotopomer Stretching Frequencies for cyclic C_5^+ in an Argon Matrix.[a]

Observed ν/cm^{-1}	Calculated ν/cm^{-1}	Difference $\Delta\nu/cm^{-1}$	Structure of Isotopomer[b]	Stat. Wts.
2052.25	2052.40	-0.15	12-12-12-12-12	1
2040.00	2039.41	0.59	13-12-12-12-12	5
2038.50	2036.60	1.90	13-12-13-12-12	5
2025.75	2025.80	-0.05	13-12-13-13-12	5
2000.50	2000.46	0.04	13-13-12-12-12	5
1988.00	1989.79	-1.79	13-13-13-12-12	5
1986.50	1986.51	-0.01	12-13-13-13-13	5
1973.25	1971.88	1.37	13-13-13-13-13	1

[a]Force constants found: f_R=17.0937 mdyn/Å, f_θ=0.2776 mdyn/Å, f_{RR}^{A}=3.1668 mdyn/Å, f_{RR}^{NA}=2.0966 mdyn/Å, $f_{R\theta}^{A}$=-0.2169 mdyn/Å and $f_{R\theta}^{NA}$=-1.3215 mdyn/Å where R and θ refer to bond stretch and internal angle bend, respectively, RR refers to adjacent (superscript A) or nonadjacent (superscript NA) bond stretch-stretch interaction and Rθ to adjacent (A) or nonadjacent (NA) bond stretch-angle bend interaction.

[b]Overall structure is a D_{5h} ring. Imagine the 2 "ends" of the structure listed in the table to be bonded.

Discussion

Evidence has been presented above that the 2052 cm^{-1} IR band is due to the planar pentagonal C_5^+ cluster. This band is not one of the more prominent bands observed when laser-vaporized graphite products are trapped in argon matrices. Yet, upon annealing the band grows to a sizable intensity. This suggests that that its growth is the result of the reaction of two smaller species, either in the warmed (30-36K) matrix, or in the plasma just after vaporization. Two possibilities are: $C_2^+ + C_3 \rightarrow C_5^+$ or $C_2 + C_3^+ \rightarrow C_5^+$. Large quantities of C_3 are known to be present in the matices and their quantity does decrease upon annealing. C_2^+ has been observed in matrices[139] but its relative quantity is, of course, unknowable via infrared spectroscopy. The second possible mechanism is more difficult to assess since IR bands due to C_3^+ have not yet been located although C_2 is probably present to a significant degree. It is known that C_3 has a lower ionization potential than C_2. The observed fragmentation[137] of C_5^+ into C_3^+ and C_2 can thus be nicely rationalized.[79] The inverse process, the formation of C_5^+ from C_3^+ and C_2, may therefore be the favoured pathway. One possible scenario for a stepwise mechanism is shown in Figure 5.3. The final ring structure shown is presumably one of five possible resonance forms resulting in five equal

Figure 5.3

Proposed mechanism for the formation of cyclic C_5^+.

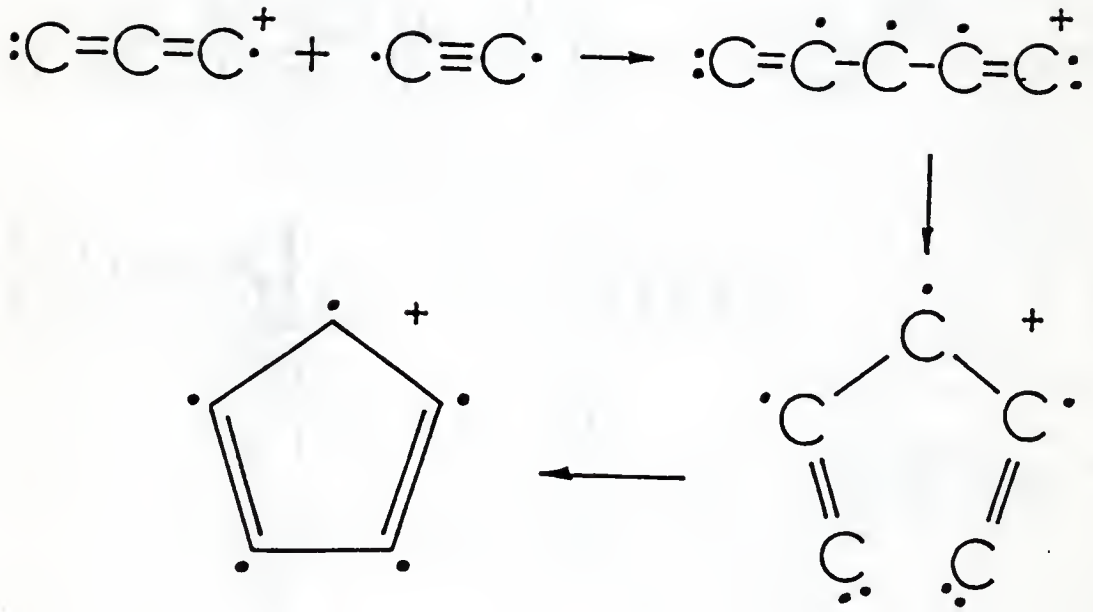

bond lengths and total D_{5h} symmetry. The matrix would probably serve to stabilize this reactive species.

It is tempting to speculate on the formation of larger clusters using the cyclic C_5^+ moeity as the template. Given the quantities of C_2 usually present in vaporized carbon mixtures, the reaction might proceed in the manner shown in Figure 5.4. With the simple addition of C_2 and C_3 clusters to the original C_5^+ ring, fused five- and six-membered ring clusters can be synthesized with the final step resulting in the bowl-shaped corannulene decaradical.

Further additions of C_2 and C_3 species would then lead to the larger clusters and possibly also to the icosahedral C_{60} cluster (Buckminsterfullerene) shown in Figure 5.5 or soot particles. Clearly, other mechanisms can also be envisaged which could lead to the same products. Kroto and McKay[152] have proposed a carbon nucleation scheme involving a corannulene framework which results in quasi-single crystal particles of concentric, spiral-shell internal structure and overall quasi-icosahedral shape composed entirely of sp_2 hybridized carbons.

Conclusion

It has been shown that the 2052 cm^{-1} band is due to a cation. The carrier of that band was then identified as C_5^+ from mixed isotope studies and normal coordinate analysis.

Figure 5.4

Proposed mechanism for the formation of the corannulene decaradical using cyclic C_5^+, C_2 and C_3 as precursors.

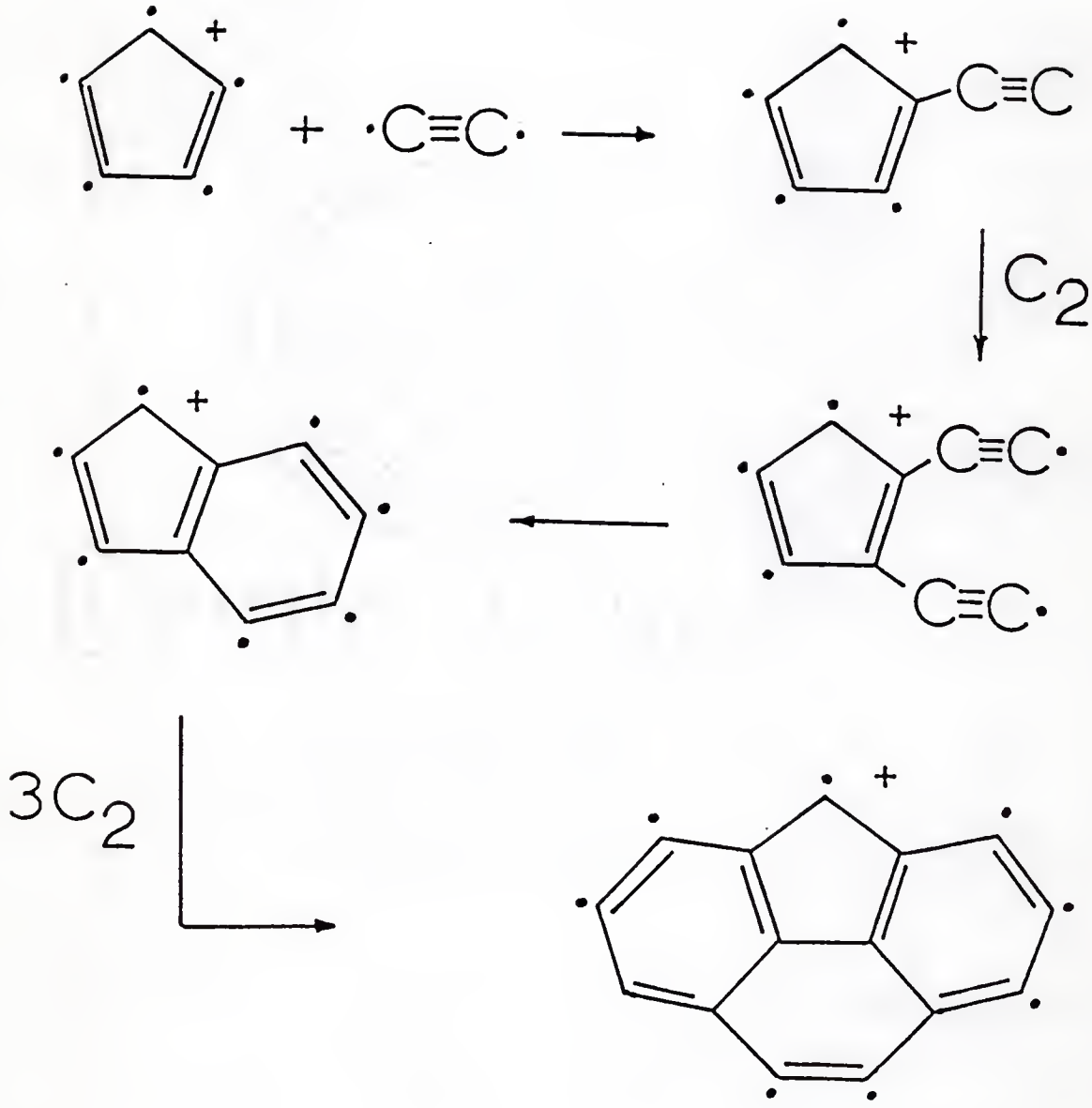
+
+ ·C≡C·
C≡C
C2
C≡C·
C≡C·
3C2

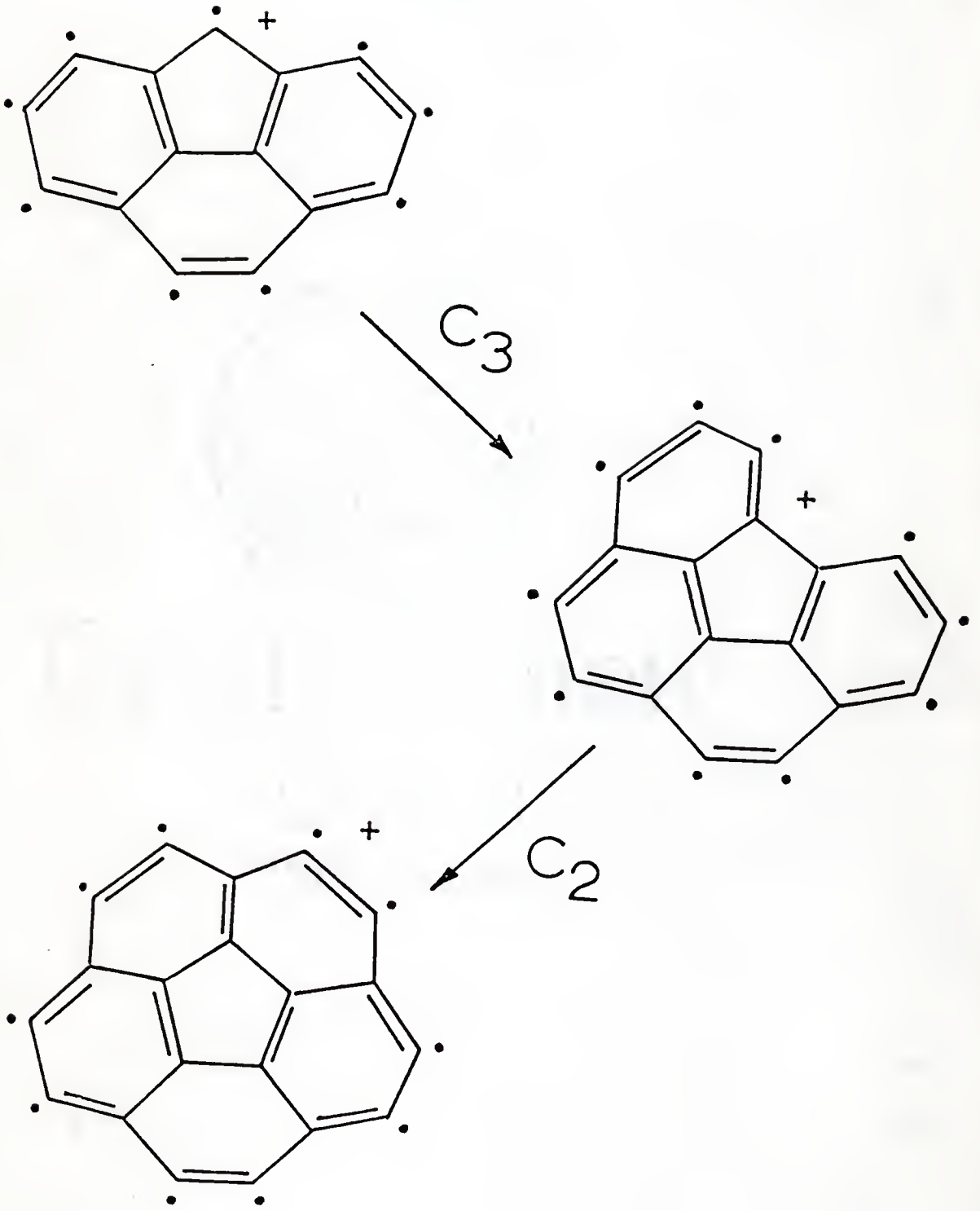

Figure 5.4 (continued)

Figure 5.5

Proposed structure of C_{60} (Buckminsterfullerene).

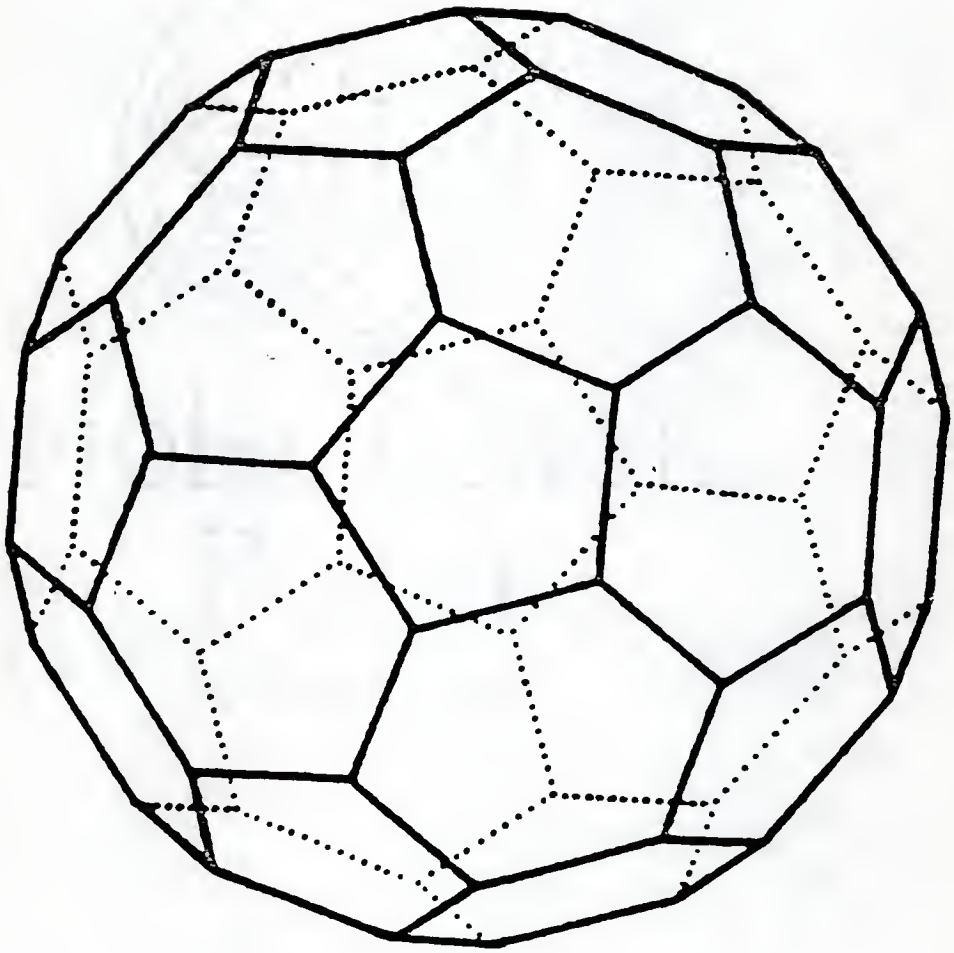

The formation of the C_5^+ ion in an argon matrix raises the interesting possibility of other ions being present in the matrix as well.

CHAPTER VI

CONCLUSIONS AND FUTURE WORK

Future Work

An interesting outcome of this study has been the assignment of the 2052 cm^{-1} band to the C_5^+ ion. Formation of C_5^+ via a completely different pathway is necessary to confirm this assignment. A fascinating series of experiments was recently reported by Lifshitz, Peres and Agranat[181] on the generation of carbon cluster ions C_n^+ by dissociative electron impact ionization of overcrowded perchloro hydrocarbons. The ions were studied by MS/MS methods including mass analysed ion kinetic energy (MIKE) spectra and kinetic energy releases (KER), collisionally activated dissociation (CAD), and charge stripping. 1,1 Bis(1,2,3,4,5-pentachlorocyclo-pentadienyl) or $C_{10}Cl_{10}$ was found to cleave at the central carbon(sp^3)-carbon(sp^3) bond to form $C_5Cl_5^+$. MIKE spectra of the $C_{10}Cl_{10}^+$ ion detected the reaction sequence shown below.

$$C_{10}Cl_{10}^+ \rightarrow C_5Cl_5^+ \rightarrow C_5Cl_4^+ \rightarrow C_5Cl_3^+ \rightarrow C_5Cl_2^+ \rightarrow C_5Cl^+ \rightarrow C_5^+.$$

It is not clear from the mass spectra whether the cyclic goemetry of the $C_5Cl_5^+$ is preserved through each step of chlorine elimination, resulting in the cyclic C_5^+ ion.

It would be desirable to determine if the C_5^+ ion produced by the above scheme is indeed cyclic. The ion could probably be produced by the VUV photolysis of $C_{10}Cl_{10}$. The experiment would consist of studying the infrared spectrum of matrix isolated $C_{10}Cl_{10}$ in argon. The appearance of the 2052 cm^{-1} band after photolysis with VUV radiation would provide strong support for the cyclic structure of C_5^+. It is suggested that an experiment along these lines would allow one to generate the C_5^+ ion by an alternate route and verify the cyclic structure of the ion.

Very little is known about the spectroscopy of carbon cluster ions. Central to the study of ions is the ability to discriminate between ions and the more numerous neutrals. One way to accomplish this would be to separate the ions from the neutrals by using a quadrupole. A quadrupole may be used to mass select specific ions and matrix isolate them for study by optical (UV/VIS, IR) and other methods. In order to better characterize the ions produced upon laser vaporization, it is suggested that such a quadrupole be built and incorporated into the matrix isolation apparatus. The quadrupole should be small enough to allow it to be bolted to the side of the displex shroud.

The extreme hardness, excellent thermal conductivity, and optical properties of diamond has made the subject of thin diamond films a very active one in recent years.[182-184] Chemical vapour deposition (CVD) is one of the more promising methods utilized in growing these films. Thin film deposition from microwave plasmas of a mixture of methane and hydrogen has been one of the more sucessful approaches in growing these films.

The detection of ions in laser-vaporized graphite is evidence for the presence of a plasma in the vaporization region. The properties of this plasma could possibly be similar to the microwave plasmas used in the CVD studies. It would be interesting to investigate the results of introducing hydrogen or a mixture of hydrogen and argon in this plasma and depositing the products on a suitable substrate such as silicon or nickel. Raman spectroscopy has been shown to be a powerful technique in characterizing diamond and diamond-like films.[185,186] Diamond is characterized by the presence of a sharp Raman band at 1332 cm^{-1}. The deposition of laser-vaporized carbon vapour mixed with hydrogen on a cold nickel block would be a logical experiment to perform. The copper window holder could be replaced by a nickel block for Raman studies. The holder could be cooled or maintained at room temperature.

Concluding Remarks

Infrared spectroscopy coupled with mixed-isotope studies and normal-coordinate analysis has been shown to be a powerful technique in elucidating the structures of small clusters. The 2164 cm^{-1}, 2052 cm^{-1}, 1998 cm^{-1} and 1952 cm^{-1} bands have been assigned to linear C_5, cyclic C_5^+, chain-like C_8 and chain-like C_6, respectively.

The limitations of this technique also became evident in the case of C_8. For linear clusters, the number of isotopomers increases very rapidly with increasing cluster size, until the isotopomer bands become so closely spaced, that a meaningful fit to calculated frequencies no longer becomes possible.

The richness of the infrared spectrum of matrix isolated, laser-ablated graphite is testament to the complex composition of the vapour and the processes that generate the species in it. Very few of these bands have been assigned to specific clusters. Clearly, there is much that remains unknown about the structure and properties of carbon clusters, especially the larger clusters. The properties of cluster ions is another largely unexplored area where much remains to be learned. The selective separation and collection of cluster ions should permit a better understanding of the spectroscopy of these important molecules.

REFERENCES

1. J.B. Edwards, "Combustion: Formation and Emission of Trace Species", Ann Arbor Sciences, Ann Arbor, 1974.

2. (a) E.A. Ballick and D.A. Ramsey, J. Chem. Phys. 29, 1418 (1958); (b) Astrophys. J. 137, 84 (1963).

3. K.H. Hinkle, J.J. Keady, P.F. Bernath, Science 241, 1319 (1988).

4. W. Weltner, Jr. and R.J. Van Zee, Chem. Rev. 89, 1713 (1989).

5. (a) W.A. Chupka and M.G. Inghram, J. Chem. Phys. 21, 371 (1953); (b) ibid. 21, 1313 (1953).

6. R.E. Honig, ibid. 22, 126 (1954).

7. J. Berkowitz and W.A. Chupka, ibid. 40, 2735 (1964).

8. J. Drowart, R.P. Burns, G. DeMaria and M.G. Inghram J. Chem. Phys. 31, 1131 (1959).

9. N. Furstnau, F. Hillenkamp and R. Nitsche, Int. J. Mass Spec. and Ion Spec. 31, 85 (1979).

10. N. Furstnau and F. Hillenkamp, ibid. 37, 135 (1981).

11. E.A. Rohlfing, D.M. Cox and A. Kaldor, J. Chem. Phys. 81, 3322 (1984).

12. G. Herzberg, Astrophys. J. 96, 314 (1942).

13. (a) A.E. Douglas, Astrophys. J. 114, 466 (1951); (b) K. Clusius and A.E. Douglas, Can. J. Phys. 32, 319 (1954).

14. R.L. Altman, J. Chem. Phys. 32, 615 (1960).

15. (a) L. Gausset, G. Herzberg, A. Lagerqvist and B. Rosen, Astrophys. J. 142, 45 (1965); (b) Disc. Faraday Soc. 35, 113 (1963).

16. (a) W. Weltner, Jr.,and P.N. Walsh, J. Chem. Phys. 37, 1153 (1962); (b) W. Weltner, Jr., P.N. Walsh and C.L. Angell, ibid. 40, 1299 (1964).

17. (a) W. Weltner, Jr. and D. McLeod, Jr., J. Chem. Phys. 40, 1305 (1964); (b) ibid. 45, 3096 (1966).

18. (a) R.L. Barger and H.P. Broida, J. Chem. Phys. 37, 1152 (1962); (b) ibid. 43, 2364 (1965).

19. G.W. Lemire, Z. Fu, I.M. Hamrick, S. Taylor and M.D. Morse, J. Phys. Chem. 93, 2313 (1989).

20. (a) P. Swings, C.T. Elvey and H.W. Babcock, Astrophys. J. 94, 320 (1941); (b) P. Swings, Rev. Mod. Phys. 14, 190 (1942); (c) B. Rosen and P. Swings, Ann. Astrophys., 16, 82 (1953).

21. (a) A. McKellar, Astrophys. J. 108, 453 (1948); (b) A. McKellar and E.H. Richardson, Mem. Soc. Roc. Sci. Liege 15, 256 (1955).

22. P. Swings, A. McKellar and K.N. Rao, Mon. Not. R. Astronom. Soc., 113, 571 (1953).

23. D. Crampton, A.P. Cowley and R.M. Humphrey, Astrophys. J. 198, L135 (1975).

24. G. Herzberg and A. Lagerqvist, Can. J. Phys. 46, 2363 (1968).

25. M. Nicol, M.L. Johnson and N.C. Holmes, Physica B + C 139-140, 582 (1986).

26. W. Huggins, Proc. R.Soc. Lond. 33, 1 (1882).

27. J.H. Callomon and D.A. Ramsey, Can. J. Phys. 35, 129 (1957).

28. A.J. Merer, ibid. 45, 4103 (1967).

29. E.A. Rohlfing and J.E.M. Goldsmith, J. Chem. Phys. 90, 6804 (1989).

30. K. Kawaguchi, K. Matsumura, H. Kanamori and E. Hirota, ibid. 91, 1953 (1989).

31. (a) R.L. Barger and H.P. Broida, J. Chem. Phys. 37, 1152 (1962); (b) ibid. 43, 2364 (1965).

32. V.E. Bondybey and J.H. English, ibid. 68, 4641 (1978).

33. G. Goldring, Y. Eisen, P. Thielberger, H.E. Wegner and A. Filevich, Phys. Rev. A26, 186 (1982).

34. I. Plesser, Z. Vager and R. Na'aman, Phys. Rev. Lett. 56, 1559 (1986).

35. Z. Vager, R. Na'aman and E.P. Kanter, Science 244, 426 (1989).

36. D.S. Gemmell, Chem. Rev. 80, 301 (1980).

37. R.O. Jones, J. Chem. Phys. 82, 5078 (1985).

38. P.R. Bunker, Ann. Rev. Phys. Chem. 34, 59 (1983).

39. R. Hoffmannn, Tetrahedron 22, 521 (1966).

40. J. Peric-Radic, J. Romelt, S.D. Peyerimhoff and R.J. Buenker, Chem. Phys. Lett. 50, 344 (1977).

41. K.P. Huber and G. Herzberg, "Molecular Spectra and Molecular Structure IV. Constants of Diatomic Molecules." Van Nostrand Reinhold, New York, 1979.

42. (a) J.O. Arnold, J. Quant. Spectrosc. Radiative Transfer 8, 1781 (1968); (b) D.M. Cooper and R.W. Nicols, ibid. 15, 139 (1975).

43. L. Brewer and L. Hagan, High Temp. Sci. 11, 233 (1979).

44. T. Tatarczyk, E.H. Fink and K.H. Becker, Chem. Phys. Lett. 40, 126 (1976).

45. (a) L. Curtis, B. Engman and P. Erman, Physica Scripta, 13, 270 (1976); (b) P.Erman, ibid. 22, 108 (1980).

46. J.D. Campbell, M.H. Yu and C. Wittig, Appl. Phys. Lett. 32, 413 (1978).

47. J.R. McDonald, A.P. Baronavski and V.M. Donnelly, Chem. Phys. 33, 161 (1978).

48. W. Bauer, K.H. Becker, M. Bielefeld and R. Meuser, Chem. Phys. Lett. 123, 33 (1986).

49. G. Theodorakopoulos, I.D. Ptesalakis, C.A. Nicolaides and R.J. Buenker, Chem. Phys. 112, 319 (1987).

50. E.F. Van Dishoeck, Chem. Phys. 77, 277 (1983).

51. C.F. Chabalowski, S.D. Peyerimhoff and R.J. Buenker, ibid. 81, 57 (1983).

52. R. Roux, D. Cerny and J. D'Incan, Astrophys. J. 204, 940 (1976).

53. S.V. O'Neil, P. Rosmos and H.J. Werner, J. Chem. Phys. 87, 2847 (1987).

54. D.M. Cooper and R.W. Nicols, J. Quant. Spectrosc. Radiative Transfer 15, 139 (1975).

55. D.M. Cooper, ibid. 26, 113 (1981).

56. A.G. Sviridov, N.N. Sobolev and M.Z. Novgorodov, ibid. 6, 337 (1966).

57. D.M. Cooper and R.W. Nicolls, Spectrosc. Lett. 9, 139 (1976).

58. D.J. DeFrees, K. Raghavachari, H.B. Schlegel and J.A. Pople, J. Am. Chem. Soc. 104, 5576 (1982).

59. K. Raghavachari, J. Chem. Phys. 82, 4607 (1985).

60. C.M. Rohlfing and R.L. Martin, J. Phys. Chem. 90, 2043 (1986).

61. A.P. Walvekar and M.A. Rama, Indian J. Phys.B 58B, 390 (1984).

62. C.W. Brown, J. Chem. Phys. 77, 5379 (1982).

63. N.E. Kuzmenko and L.V. Chumak, J. Quant. Spectrosc. Radiative Transfer 35, 419 (1986).

64. A.J. Sauval and J.B. Tatum, Astrophys. J. Suppl. Ser. 56, 193 (1984).

65. S.C. Rossi, W.J. Maciel and P. Benevides-Soares, Astronom. Astrophys. 148, 93 (1985).

66. (a) E. Clementi and H. Clementi, J. Chem. Phys. 36, 2824 (1962); (b) E. Clementi, J. Am. Chem. Soc. 83, 450 (1961).

67. K.S. Pitzer and E. Clementi, J. Am. Chem. Soc. 81, 4477 (1959).

68. J.P. Ritchie, H.F. King and W.S. Young, J. Chem. Phys. 85, 5175 (1986).

69. R.A. Whiteside, K. Raghavachari, D.J. DeFrees, J.A. Pople and P.V.R. Schleyer, Chem. Phys. Lett. 78, 538 (1981).

70. D. Michalska and H. Chojnacki, ibid. 141, 376 (1987).

71. D.E. Bernholdt, D.H. Magers and R.J. Bartlett, J. Chem. Phys. 89, 3612 (1988).

72. R.H. Sanborn, J. Chem. Phys. 49, 4219 (1968).

73. J.M.L. Martin, J.P. Francois and R. Gijbels, ibid. 90, 3403 (1989).

74. W.R.M. Graham, K.I. Dismuke and W. Weltner, Jr., Astrophys. J., 204, 301 (1976).

75. H.M. Cheung and W.R.M. Graham, ibid. 91, 6664 (1989).

76. P.S. Skell, J.J. Havel and M.J. McGlinchey, Acc. Chem. Res. 6, 97 (1973).

77. E. Clementi and A.C. McLean, J. Chem. Phys. 36, 45 (1962).

78. D.H. Magers, R.J. Harrison, R.J. Bartlett ibid. 84, 3284 (1986).

79. K. Raghavachari and J.S. Binkley, ibid. 87, 2191 (1987).

80. K. Raghavachari, R.A. Whiteside and J.A. Pople, J. Chem. Phys. 85, 6623 (1986).

81. (a) J. Bernholc and J.C. Phillips, Phys. Rev. B33, 7395 (1986); (b) J. Chem. Phys. 85, 3266 (1986).

82. D.W. Ewing and G.V. Pfeiffer, Chem. Phys. Lett. 86, 365 (1982).

83. D.W. Ewing and G.V. Pfeiffer, ibid. 134, 413 (1987).

84. D.W. Ewing and G.V. Pfeiffer, "Physics and Chemistry of Small Clusters." Eds: P.Jena, B.K.Rao, S.N.Khanna, Plenum Press, New York, 1987, p.67.

85. L.S. Ott and A.K. Ray, "Physics and Chemistry of Small Clusters." Eds: P.Jena, B.K.Rao, S.N.Khanna, Plenum Press, New York, 1987, p.95.

86. K.R. Thompson, R.L. DeKock and W. Weltner, Jr., J. Am. Chem. Soc. 93, 4688 (1971).

87. V. Parasuk and J. Almlof, J. Chem. Phys. 91, 1137 (1989).

88. W. Kratschmer, N. Sorg and D.R. Huffman, Surf. Sci. 156, 814 (1985).

89. R.J. Van Zee, R.F. Ferrante, K.J. Zeringue and W. Weltner, Jr., J. Chem. Phys. 88, 3465 (1988).

90. (a) V.E. Strel'nitskii, V.G. Padalka and S.I. Vakula, Zh. Tekh. Fiz. 48, 377 (1978),[Sov. Phys. Tech. Phys. 23, 222 (1978)]; (b) A.S. Bakai and V.E. Strel'nitskii, ibid. 51, 2414 (1981),[ibid. 26, 1425 (1981)]; (c) N.N. Matyushenko, V.E. Strel'nitskii and V.A. Gusev, Zh. Eksp. Teor. Fiz. 30, 218 (1979),[JETP Lett. 30, 199 (1979)].

91. J.K. Burdett and S. Lee, J. Am. Chem. Soc. 107, 3063 (1985).

92. R.L. Johnson and R. Hoffmann, ibid. 111, 810 (1989).

93. O. Hahn, F. Strassman, J. Mattauch and H. Ewald, Naturwiss. 30, 541 (1942).

94. J. Mattauch, H. Ewald, O. Hahn and F. Strassman, Z. Phys. 20, 598 (1943).

95. H. Hintenberger, J. Franzen and K.D. Schuy, Z. Naturforch. Teil A 18, 1236 (1963).

96. J.R. Heath, Q. Zhang, S.C. O'Brien, R.F. Curl, H.W. Kroto and R.E. Smalley, J. Am. Chem. Soc. 109, 359 (1987).

97. R.E. Palmer and M. Shelef, "The Chemistry and Physics of Carbon." Ed: P.L.Walker, Edward Arnold, London (1968), Vol. 4, p.85.

98. S.W. McElvany, B.I. Dunlap and A. O'Keefe, J. Chem. Phys. 86, 715 (1987).

99. D.C. Parent and S.W. McElvany, J. Am. Chem. Soc., 111, 2393 (1988).

100. (a) S.W. McElvany, W.R. Creasy and A. O'Keefe, J. Chem. Phys. 85, 632 (1986); (b) S.W. McElvany, ibid. 89, 2063 (1988).

101. S.H. Yang, K.J. Taylor, M.J. Craycraft, J. Conceicao, C.L. Pettiette, O. Cheshnovsky and R.E. Smalley, Chem. Phys. Lett. 144, 431 (1988).

102. H.W. Kroto, J.R. Heath, S.C. O'Brien, R.F. Curl and R.E. Smalley, Nature 318, 162 (1985).

103. Q.L. Zhang, S.C. O'Brien, J.R. Heath, Y. Liu, R.F. Curl, H.W. Kroto and R.E. Smalley, J. Phys. Chem. 90, 525 (1986).

104. H.W. Kroto, Nature 329, 529 (1987).

105. D.W. Thompson, "On Growth and Form." Cambridge University Press. London, 1942.

106. D.J. Klein, T.G. Schmalz, G.E. Hite and W.A. Seitz, J. Am. Chem. Soc. 108, 1301 (1986).

107. D.M. Cox, K.C. Reichmann and A. Kaldor, J. Chem. Phys. 88, 1588 (1988).

108. S.C. O'Brien, J.R. Heath, R.F. Curl and R.E. Smalley, ibid. 88, 220 (1988).

109. D.E.H. Jones, New Scientist, Nov. 3, 245 (1966).

110. J.R. Heath, S.C. O'Brian, Q. Zhang, Y. Liu, R.F. Curl, H.W. Kroto, F.K. Tittel and R.E. Smalley, J. Am. Chem. Soc. 107, 7779 (1985).

111. F.D. Weiss, J.L. Elkind, S.C. O'Brien, R.F. Curl and R.E. Smalley, J. Am. Chem. Soc. 110, 4464 (1988).

112. S.H. Yang, C.L. Pettiette, J. Conceicao, O. Cheshnovsky and R.E. Smalley, Chem. Phys. Lett. 139, 233 (1987).

113. J.R. Heath, R.F. Curl and R.E. Smalley, J. Chem. Phys. 87, 4236 (1987).

114. S. Larsson, A. Volosov and A. Rosen, Chem. Phys. Lett. 137, 501 (1987).

115. D.N. Lineman, K.V. Somayajula, A.G. Sharkey and D.M. Hercules, J. Phys. Chem. 93, 5025 (1989).

116. A. O'Keefe, M.M. Ross and A.P. Baronavski, Chem. Phys. Lett. 130, 17 (1986).

117. M. Ozaki and A. Takahashi, ibid. 127, 242 (1986).

118. (a) R.C. Hadden, L.E. Brus and K. Raghavachari, Chem. Phys. Lett. 125, 459 (1986); (b) ibid. 131, 165 (1986).

119. T.G. Schmalz, W.A. Sietz, D.J. Klein and G.E. Hite, ibid. 130, 203 (1986).

120. S. Satpathy, ibid. 130, 545 (1986).

121. D.S. Marynick and S. Estreicher, ibid. 132, 338 (1986).

122. P.W. Fowler and J. Woolrich, ibid. 127, 78 (1986).

123. I. Laszlo and L. Udvardi, ibid. 136, 418 (1987).

124. T.I. Shibuya and M. Yoshitani, ibid. 137, 13 (1987).

125. G.W. Hayden and E.J. Mele, Phys. Rev. B36, 5010 (1987).

126. D.J. Klein, W.A. Seitz and T.G. Schmalz, Nature 323, 703 (1986).

127. A. Otto, Z. Chem. 10, 380 (1987).

128. M.D. Newton and R.E. Stanton, J. Am. Chem. Soc. 108, 2469 (1986).

129. P.D. Hale, ibid. 108, 6087 (1986).

130. M.L. McKee and W.C. Herndon, J. Mol. Struct.(Theochem) 153, 75 (1987).

131. (a) R.L. Disch and J.M. Sclulman, Chem. Phys. Lett. 125, 465 (1986); (b) J.M. Schulman, R.L. Disch, M.A. Miller and R.C. Peck, ibid. 141, 45 (1987).

132. H.P. Luthi and J. Almlof, ibid. 135, 357 (1987).

133. C. Coulombeau and A. Rassat, J. Chim. Phys. 84, 875 (1987).

134. Z.C. Wu, D.A. Jelski and T.F. George, Chem. Phys. Lett. 144, 366 (1988).

135. D.E. Weeks and W.G. Harter, ibid. 144, 366 (1988).

136. L.A. Bloomfield, M.E. Geusic, R.R. Freeman and W.L. Brown, Chem. Phys. Lett. 121, 33 (1985).

137. (a) M.E. Geusic, T.J. McIlrath, M.F. Jarrold, L.A. Bloomfield, R.R. Freeman and W.L. Brown, J. Chem. Phys. 84, 2421 (1986); (b) M.E. Geusic, M.F. Jarrold, T.J. McIlrath, R.R. Freeman and W.L. Brown, ibid. 86, 3862 (1987).

138. A. O'Keefe, R. Derai and M.T. Bowers, Chem. Phys. 91, 161 (1984).

139. D. Forney, H. Althaus and J.P. Maier, J. Phys Chem. 91, 6458 (1987).

140. M. Rosslein, M. Wyttenbach and J.P. Maier, J. Chem. Phys. 87, 6770 (1987).

141. J.P. Maier and M. Rosslein, ibid. 88, 4614 (1988).

142. W.C. Lineberger and T.A. Patterson, Chem. Phys. Lett. 13, 40 (1972).

143. P.L. Jones, R.D. Mead, B.E. Kohler, S.D. Rosner and W.C. Lineberger, J. Chem. Phys. 73, 4419 (1980).

144. R.D. Mead, K.R. Lykke, W.C. Lineberger, J. Marks and J.I. Brauman, ibid. 81, 4883 (1984).

145. K.R. Lykke, R.D. Mead and W.C. Lineberger, Phys. Rev. Lett. 52, 2221 (1984).

146. R.D. Mead, U. Hefter, P.A. Schulz and W.C. Lineberger, J. Chem. Phys. 82, 1723 (1985).

147. (a) B.D. Rehfuss, D.J. Liu, B.M. Dinelli, M.F. Jagod, W.C. Ho, M.W. Crofton and T. Oka, J. Chem. Phys. 89, 129 (1988); (b) T. Oka, Phil. Trans. R. Soc. Lond. A 324, 81 (1988).

148. D.E. Milligan and M.E. Jacox, J. Chem. Phys. 51, 1952 (1969).

149. R.P. Frosch, ibid. 54, 2660 (1971).

150. S.J. Harris and A.M. Weiner, Ann. Rev. Phys. Chem. 36, 31 (1985).

151. P.H. Gerhardt, S. Loffler and K.H. Homann, Chem. Phys. Lett. 137, 306 (1987).

152. H.W. Kroto and K.G. McKay, Nature 331, 328 (1988).

153. S. Iijima, J. Cryst. Growth 50, 675 (1980).

154. G. Herzberg, "Molecular Spectra and Molecular Structure," Vol. 2, Infrared and Raman Spectra of Polyatomic Molecules. Van Nostrand, New York, 1945.

155. S. Suzer and L. Andrews, J. Chem. Phys 88, 916 (1988).

156. Z. Slanina and R. Zahradnik, J. Phys. Chem. 81, 2252 (1977).

157. R. Pellow and M. Vala, Zeit. Phys. D (in press).

158. E.B. Wilson, Jr., J.C. Decius and P.C. Cross, "Molecular Vibrations." Dover Publications, New York, 1945.

159. W.H. Smith and G.E. Leroi, J. Chem. Phys. 45, 1767 (1966).

160. D.E. McIntosh and M.R. Peterson, QCPE Program No. QCMP012: "General Vibrational Analysis Programs Utilizing the Wilson GF Method for a General Unsymmetrized Molecule." Quantum Chemistry Program Exchange, Indiana University.

161. L.N. Shen and W.R.M. Graham, J. Chem. Phys. 91, 5115 (1989).

162. M. Vala, T.M. Chandrasekhar, J. Szczepanski, R.V. Zee and W. Weltner, Jr., J. Chem. Phys. 90, 595 (1989).

163. P.F. Bernath, K.H. Hinkle and J.J. Keady, Science 244, 562 (1989).

164. N. Moazzen-Ahmadi, A.R.W. McKellar and T. Amano, Chem. Phys. Lett. 157, 1 (1989).

165. J.R. Heath, A.L. Cooksy, M.H.W. Gruebele, C.A. Schmuttenmaer and R.J. Saykally, Science 244, 564 (1989).

166. "Lange's Handbook of Chemistry," 13th ed. Ed: J.A. Dean, McGraw-Hill Book Company, New York, 1985.

167. W. Kratschmer and K. Nachtigall, "Polycyclic Aromatic Hydrocarbons and Astrophysics.", Eds: A. Leger, L. d'Hendecourt and N. Boccara, D. Reidel Publishing Company, Dordrecht, Holland, 1989, p.75.

168. M. Vala, T.M. Chandrasekhar, J. Szczepanski and R. Pellow, High Temp. Sci. (in press).

169. J.O. Halford, J. Chem. Phys. 19, 1375 (1951).

170. V.E. Dornenburg, H. Hintenberger and J. Franzen, Z. Naturforch 16, 532 (1961).

171. P.J.M. Leleyter, J. Physique 45, 1681 (1984).

172. R.A. Whiteside, R. Krishnan, M.J. Frisch, J.A. Pople and P.V.R. Schleyer, Chem. Phys. Lett. 80, 547 (1981).

173. W.L. Brown, R.R. Freeman, K. Raghavachari and M. Schluter, Science 235, 860 (1987).

174. P.P. Radi, T.L. Bunn, P.R. Kemper, M.E. Molchan and M.T. Bowers, J. Chem. Phys. 88, 2809 (1988).

175. M.S. Islam and A.K. Ray, J. Phys. B 22, 2071 (1989).

176. L.E. Brus and V.E. Bondybey, J. Chem. Phys. 63, 3123 (1975).

177. (a) L. Andrews, Appl. Spectrosc. Rev. 11, 125 (1976). (b) L. Andrews, Ann. Rev. Phys. Chem. 30, 79 (1979).

178. M.E. Jacox, Rev. Chem. Intermed. 1, 1 (1978).

179. (a) T.A. Miller and V.E. Bondybey, J. Chim. Phys. 77, 695 (1980); (b) Appl. Spectrosc. Rev. 18, 105 (1982).

180. V.E. Bondybey and L.E. Brus, Adv. Chem. Phys. 41, 269 (1980).

181. C. Lifshitz, T. Peres and I. Agranat, Int. J. Mass Spectrom. Ion Proc. 93, 149 (1989).

182. (a) J.C. Angus, Thin Solid Films 142, 145 (1986). (b) J.C. Angus and C.C. Hayman, Science 241, 913 (1988).

183. R.C. DeVeies, Ann. Rev. Mater. Sci. 17, 161 (1987).

184. J.C. Angus and F. Jansen, J. Vac. Sci. Technol. A 6, 1778 (1988).

185. A.V. Baranov and E.A. Konshina, Opt. Spectrosc.(USSR) 65, 506 (1988).

186. R.O. Dillon and J.A. Woollam, Phys. Rev. B 29, 3482 (1984).

BIOGRAPHICAL SKETCH

T. M. Chandrasekhar was born on February 24, 1961, in Poona, India. He attended Loyola High School in Poona and graduated in 1978. He later attended the Indian Institutes of Technology at Kharagpur and Bombay pursuing a major in chemisty. After receiving an M.Sc. in chemistry in the spring of 1984, he came to the University of Florida to pursue a Ph.D. in physical chemistry.

I certify that I have read this study and that in my opinion it conforms to acceptable standards of scholarly presentation and is fully adequate, in scope and quality, as a dissertation for the degree of Doctor of Philosophy.

Martin T. Vala, Chairman
Professor of Chemistry

I certify that I have read this study and that in my opinion it conforms to acceptable standards of scholarly presentation and is fully adequate, in scope and quality, as a dissertation for the degree of Doctor of Philosophy.

William Weltner, Jr.
Professor of Chemistry

I certify that I have read this study and that in my opinion it conforms to acceptable standards of scholarly presentation and is fully adequate, in scope and quality, as a dissertation for the degree of Doctor of Philosophy.

Vaneica Young
Associate Professor of Chemistry

I certify that I have read this study and that in my opinion it conforms to acceptable standards of scholarly presentation and is fully adequate, in scope and quality, as a dissertation for the degree of Doctor of Philosophy.

Samuel O. Colgate
Associate Professor of Chemistry

I certify that I have read this study and that in my opinion it conforms to acceptable standards of scholarly presentation and is fully adequate, in scope and quality, as a dissertation for the degree of Doctor of Philosophy.

Clifford T. Johnston
Assistant Professor of Soil Science

This dissertation was submitted to the Graduate Faculty of the Department of Chemistry in the College of Liberal Arts and Sciences and to the Graduate School, and was accepted as partial fulfillment of the requirements for the degree of Doctor of Philosophy.

May, 1990

Dean, Graduate School

UNIVERSITY OF FLORIDA
3 1262 08556 9951